materials

MDPI

Review

Recent Advances of Indium Oxide-Based Catalysts for CO_2 Hydrogenation to Methanol: Experimental and Theoretical

Dongren Cai *, Yanmei Cai, Kok Bing Tan and Guowu Zhan *

Integrated Nanocatalysts Institute (INCI), College of Chemical Engineering, Huaqiao University, 668 Jimei Avenue, Xiamen 361021, China

* Correspondence: 15506@hqu.edu.cn (D.C.); gwzhan@hqu.edu.cn (G.Z.)

Abstract: Methanol synthesis from the hydrogenation of carbon dioxide (CO_2) with green H_2 has been proven as a promising method for CO_2 utilization. Among the various catalysts, indium oxide (In_2O_3)-based catalysts received tremendous research interest due to the excellent methanol selectivity with appreciable CO_2 conversion. Herein, the recent experimental and theoretical studies on In_2O_3-based catalysts for thermochemical CO_2 hydrogenation to methanol were systematically reviewed. It can be found that a variety of steps, such as the synthesis method and pretreatment conditions, were taken to promote the formation of oxygen vacancies on the In_2O_3 surface, which can inhibit side reactions to ensure the highly selective conversion of CO_2 into methanol. The catalytic mechanism involving the formate pathway or carboxyl pathway over In_2O_3 was comprehensively explored by kinetic studies, in situ and ex situ characterizations, and density functional theory calculations, mostly demonstrating that the formate pathway was extremely significant for methanol production. Additionally, based on the cognition of the In_2O_3 active site and the reaction path of CO_2 hydrogenation over In_2O_3, strategies were adopted to improve the catalytic performance, including (i) metal doping to enhance the adsorption and dissociation of hydrogen, improve the ability of hydrogen spillover, and form a special metal-In_2O_3 interface, and (ii) hybrid with other metal oxides to improve the dispersion of In_2O_3, enhance CO_2 adsorption capacity, and stabilize the key intermediates. Lastly, some suggestions in future research were proposed to enhance the catalytic activity of In_2O_3-based catalysts for methanol production. The present review is helpful for researchers to have an explicit version of the research status of In_2O_3-based catalysts for CO_2 hydrogenation to methanol and the design direction of next-generation catalysts.

Keywords: CO_2 hydrogenation; methanol; indium oxide-based catalysts; oxygen vacancies; hydrogen dissociation

Citation: Cai, D.; Cai, Y.; Tan, K.B.; Zhan, G. Recent Advances of Indium Oxide-Based Catalysts for CO_2 Hydrogenation to Methanol: Experimental and Theoretical. *Materials* **2023**, *16*, 2803. https://doi.org/10.3390/ma16072803

Academic Editor: Juan M. Coronado

Received: 26 February 2023
Revised: 20 March 2023
Accepted: 23 March 2023
Published: 31 March 2023

1. Introductions

The greenhouse effect caused by excessive CO_2 emission has seriously threatened the survival of human beings and other organisms [1–4]. In order to cope with the current grim situation, many countries have established a target timeline to reach the peak of CO_2 emission and achieve carbon neutrality. For example, China has promised to realize a carbon peak by 2030 and carbon neutrality by 2060 [5–8]. Therefore, CO_2 capture and utilization (CCU) technology has attracted much attention [9–13]. In particular, the use of "green hydrogen" produced with renewable energy to convert waste CO_2 into methanol is not only able to effectively reduce CO_2 emission but also can store renewable energy in liquid fuel, which is an important method to realize resource utilization of CO_2 [14–19].

CO_2 hydrogenation to methanol mainly includes CO_2 to methanol reaction (1), reverse water gas shift reaction (RWGS, 2), and CO to methanol reaction (3), respectively [20–23]. Reactions (1) and (3) are exothermic; thus, low temperature is conducive to the formation of methanol but hinders the activation of CO_2. On the contrary, competitive reaction (2) is an endothermic reaction, which is significantly promoted at high temperatures,

resulting in a sharp decrease in methanol selectivity [24–26]. Therefore, the development of efficient catalysts with the aim to decrease CO_2 activation energy and promote methanol formation at a suitable temperature is the key to realizing the industrial application of CO_2 hydrogenation to methanol.

$$CO_2 + 3H_2 \leftrightarrows CH_3OH + H_2O \quad \Delta H_{298\,K} = -49.5\ kJ/mol \tag{1}$$

$$CO_2 + H_2 \leftrightarrows CO + H_2O \quad \Delta H_{298\,K} = 41.2\ kJ/mol \tag{2}$$

$$CO + 2H_2 \leftrightarrows CH_3OH \quad \Delta H_{298\,K} = -90.7\ kJ/mol \tag{3}$$

Currently, several types of materials have been used as the catalysts for CO_2 hydrogenation to methanol, including Cu [15,27–29], noble metals (Pt, Pd, Ru, etc.) [30–33], M_aZrO_x (M_a = Ga, Zn, etc.) solid solution [34–37], and indium oxide (In_2O_3) [21,38–40]. Among them, Cu-based catalysts have been widely investigated in CO_2 hydrogenation to methanol [41]. However, they are prone to the Ostwald ripening effect and particle migration under high temperatures and water surroundings, which results in catalyst deactivation [42–44]. By comparison, noble metals exhibit high stability and resistance to sintering and poisoning, so they are regarded as an alternative to Cu-based catalysts. Nevertheless, these catalysts are not able to efficiently catalyze the reaction and regulate the product distribution due to the weak binding with CO_2 molecules [45,46]. Our previous research also confirmed this conclusion, which reveals that when Pt catalyzes CO_2 hydrogenation alone, no methanol generates, and the selectivity of CO is as high as 100% [5,47]. Moreover, M_aZrO_x solid solution, particularly $ZnZrO_x$, is a potential catalyst for CO_2 hydrogenation to methanol [35,48–50]. In $ZnZrO_x$, Zn is doped into ZrO_2 lattice by replacing Zr (Zn-Zr-O_x), and the solid solution structure provides reaction sites of Zn and adjacent Zr for activating H_2 and CO_2, respectively (synergistic effect), thus producing methanol with high selectivity [51]. However, the low activity and the mobility of ZnO still limit the applications of the catalysts [36].

To our knowledge, In_2O_3 has been regarded as a highly selective catalyst for CO_2 hydrogenation to methanol in recent years [52]. It is generally believed that CO_2 can be adsorbed and activated by oxygen vacancies on the In_2O_3 surface, which are periodically generated and annihilated to inhibit the occurrence of side reactions, therefore hydrogenating CO_2 to methanol with high selectivity [53–55]. Not only does In_2O_3 show higher methanol selectivity than Cu and noble metals, but it also exhibits higher catalytic activity than ZnO [21]. Additionally, In_2O_3 can be further supported and modified to promote the activation of CO_2 and H_2, and stabilize the key reaction intermediates, thus presenting great potential to become an excellent catalyst for the sustainable and efficient production of methanol. Herein, we gave a comprehensive overview of the recent advances of In_2O_3-based catalysts for CO_2 hydrogenation to methanol. The active site and mechanism of pure In_2O_3 catalyst for CO_2 hydrogenation were stated at first. Then, the discussion was concentrated on two important strategies, namely metal doping and hybrid with other metal oxides, to enhance the catalytic activity of In_2O_3 by promoting the dissociation of hydrogen to hydrogenate intermediates and the formation of oxygen vacancies to activate CO_2 and stabilize the key intermediates. Some suggestions in the future study were finally proposed to improve the performance of In_2O_3-based catalysts for CO_2 hydrogenation to methanol from the experimental and theoretical aspects. This review focused on the regulation and modification of active sites of In_2O_3-based catalysts to facilitate the activation of reactants and stabilization of intermediates in CO_2 hydrogenation, which is conducive to the design of more efficient In_2O_3-based catalysts in future studies.

2. In_2O_3-Based Catalysts for CO_2 Hydrogenation to Methanol

2.1. Pure In_2O_3 Catalyst

The idea of In_2O_3 as the catalyst for CO_2 hydrogenation to methanol stems from its excellent CO_2 selectivity in methanol steam reforming (MSR) reactions [56,57]. Based on density functional theory (DFT), Ge et al. [53] predicted the feasibility of CO_2 hydrogenation to methanol catalyzed by In_2O_3 (110) with oxygen vacancies. They proposed that In_2O_3 would inhibit RWGS reaction, and methanol was the major product on the surface of defective In_2O_3 (110). As shown in Figure 1, the reaction process obeys the mechanism of periodic generation and annihilation of oxygen vacancies, including adsorption and activation of CO_2 on oxygen vacancies, CO_2 hydrogenation to form intermediate species, methanol desorption, and regeneration of oxygen vacancies. To confirm the research results of DFT, Liu et al. [38] used commercial In_2O_3 activated at a high temperature (500 °C) as the catalyst for CO_2 hydrogenation. The experimental results demonstrated that methanol yield increased with the increase in reaction pressure; however, due to the limitation of thermodynamics, it increased first and then decreased as the temperature increased. In addition, 2.82% of methanol yield and 3.69 mol h^{-1} $kg_{cat}{}^{-1}$ of methanol production rate were obtained at 330 °C and 4 MPa, which was superior to many other catalysts. In 2016, Pérez-Ramírez et al. [58] revealed that nano In_2O_3 can efficiently catalyze CO_2 hydrogenation to methanol, obtaining more than 0.18 g_{MeOH} h^{-1} $g_{cat}{}^{-1}$ of space-time yield. They also found that compared to $Cu/ZnO/Al_2O_3$, the highest methanol yield of In_2O_3 was achieved at 300 °C, indicating that In_2O_3 can maintain high methanol selectivity at higher temperatures. Two years later, they reported the mechanism and microkinetics of methanol synthesis from CO_2 hydrogenation over In_2O_3 [59]. The results indicated that the apparent activation energy experimentally determined for CO_2 hydrogenation to methanol (103 kJ mol^{-1}) was lower than that of the RWGS reaction (117 kJ mol^{-1}), which explains the superior methanol selectivity over In_2O_3. In_2O_3 (111) was experimentally and theoretically proved to be the most exposed surface termination, indicating CO_2 can be activated by oxygen vacancies surrounded by three indium atoms. In addition, the most favorable pathway to methanol comprises three consecutive additions of hydrides and protons, which features CH_2OOH* and $CH_2(OH)_2$* as intermediates. In 2019, by an operando examination, Müller et al. [60] proved that In_2O_{3-x} was the active phase of methanol synthesis, while In^0 led to the deactivation of the catalyst.

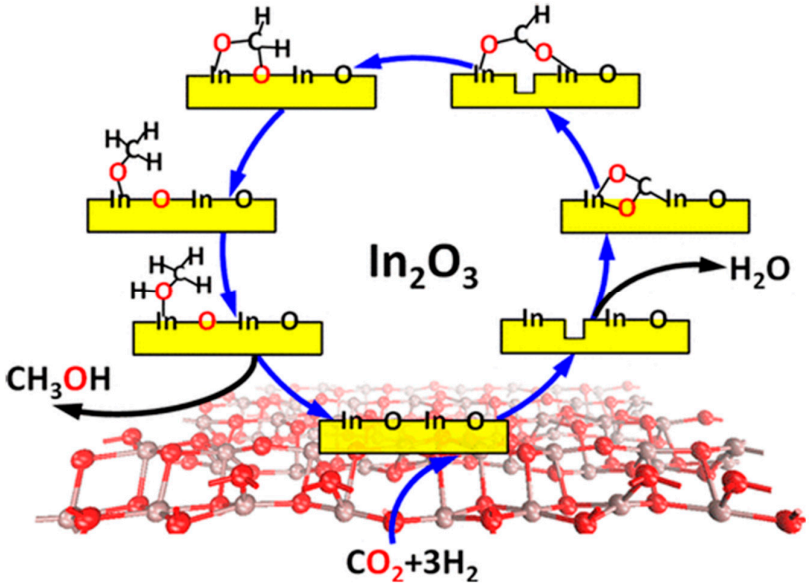

Figure 1. The active site and catalytic mechanism of CO_2 hydrogenation to methanol over defective In_2O_3 (110). Reproduced with permission from ref. [53]. Copyright 2013 American Chemical Society.

Liu et al. [61] prepared an In_2O_3 catalyst by precipitation method for CO_2 hydrogenation to methanol. The results showed that under the operating conditions (H_2/CO_2 molar ratio of 4, the volume space velocity of 21,000 $cm^3\ h^{-1}\ g_{cat}{}^{-1}$, reaction pressure of 5 MPa, and reaction temperature of 300 °C), the CO_2 conversion and methanol space-time yield were 9.4% and 0.335 $g_{MeOH}\ h^{-1}\ g_{cat}{}^{-1}$. Guo et al. [62] investigated the catalytic activity of cubic bixbyite-type indium oxide (*c*-In_2O_3) and rhombohedral corundum-type indium oxide (*r*-In_2O_3) in CO_2 hydrogenation to methanol. Due to the impressive reducibility and reactivity, *c*-In_2O_3 was higher than *r*-In_2O_3 in CO_2 conversion; however, *r*-In_2O_3 possessed higher methanol selectivity because of weaker methanol and stronger CO adsorption. Moreover, the in situ DRIFTS experiments revealed that CO_2 could be reduced to CO via redox cycling and hydrogenated to methanol via the formate pathway. In addition, Sun et al. [63] successfully designed an In_2O_3 nanocatalyst with higher catalytic activity under the guidance of theoretical calculation, which suggested that the hexagonal In_2O_3 (104) surface had a far superior catalytic performance. As shown in Figure 2, the experimental results also confirmed that compared to cubic In_2O_3 (*c*-In_2O_3), a novel hexagonal In_2O_3 (*h*-In_2O_3-R) with a high proportion of the exposed (104) surface exhibited higher catalytic activity and possessed high stability. Moreover, Li et al. [54] investigated the dissociative adsorption of H_2 during CO_2 hydrogenation over cubic and hexagonal In_2O_3 by DFT, and they found that the oppositely charged In and O pair sites on the reduced In_2O_3 surfaces played a significant role in facilitating the heterolytic dissociation of H_2, which contributed to the formation of anionic hydride around the In sites to promote CO_2 hydrogenation to methanol. Additionally, *h*-In_2O_3 (104) surface is considered the best surface for CO_2 hydrogenation to methanol due to the facile formation of the oxygen vacancies at low coverage and the favorable formation of the hydride adsorbate at the In sites.

In the last two years, the research topic of CO_2 hydrogenation to methanol over In_2O_3 has still attracted considerable interest. Based on the solvothermal method, Wu et al. [64] successfully fabricated mixed-phase indium oxide with controllable cubic and hexagonal phases to enhance catalytic performance in CO_2 hydrogenation to methanol. Due to its enhanced textural properties and oxygen vacancies, mixed-phase *c*/*h*-In_2O_3 catalysts demonstrated higher CO_2 conversion and space-time yield of methanol and kept stable in the reaction. To understand the structure–activity relationship, Nørskov et al. [65] systematically studied the methanol synthesis over In_2O_3 (111) and In_2O_3 (110) by combining DFT calculations with microkinetic modeling. The theoretical activity volcano shown in Figure 3 suggested that catalytic activity was closely related to the number of reduced In layers on In_2O_3 surfaces, specifically, for In_2O_3 (110), a surface oxygen vacancies between 0.17 and 1 ML (ML: the top layer, from surface to interior) possessed the highest catalytic activity, while for In_2O_3 (111), the number of oxygen vacancies should be increased to 1~5 ML to obtain the optimal activity. Similarly, Gao et al. [66] revealed the structure–performance relationship of cubic In_2O_3 catalyst in CO_2 hydrogenation via the study of reaction mechanism and catalytic activities at all the different surface oxygen vacancy sites on stable (111) flat surface, (110) flat surface, and (110) step surface. The conclusion was that the rate-determining step of methanol synthesis for a given oxygen vacancy site can be determined by the stability of H_2COO* and CH_2O* intermediates along with the formation energy of the oxygen vacancy sites, and tri-coordinated oxygen vacancy sites were beneficial to the formation of methanol, whereas bi-coordinated oxygen vacancy sites favor CO formation. CO_2 hydrogenation to methanol on indium-terminated In_2O_3 (100), defective In_2O_3 (110), and In_2O_3 (111) surfaces were also deeply investigated by Zhang et al. [67]. It was found that the adsorbed CO_2 was preferable to form HCOO* compared with CO* and COOH* and underwent HCOO*, H_2CO*, and H_3CO* intermediates due to the lowest energy barriers. The defective In_2O_3 (110) was proven to be the optimal surface for CO_2 hydrogenation to methanol, while the indium-terminated In_2O_3 (100) surface displayed the lowest catalytic activity. In addition, Creaser et al. [39] proposed a kinetic model based on Langmuir–Hinshelwood–Hougen–Watson (LHHW) mechanism for CO_2 hydrogenation to methanol over In_2O_3 catalyst. The model revealed that RWGS

was obviously enhanced at high temperatures, causing methanol synthesis to reverse (methanol steam reforming, MSR). Apparent activation energies for CO_2 hydrogenation to methanol and RWGS were 90 and 110 kJ mol^{-1}, respectively, over In_2O_3 derived from the experimental data. The results obtained from these detailed investigations were conducive to the development of reliable reactor and process designs.

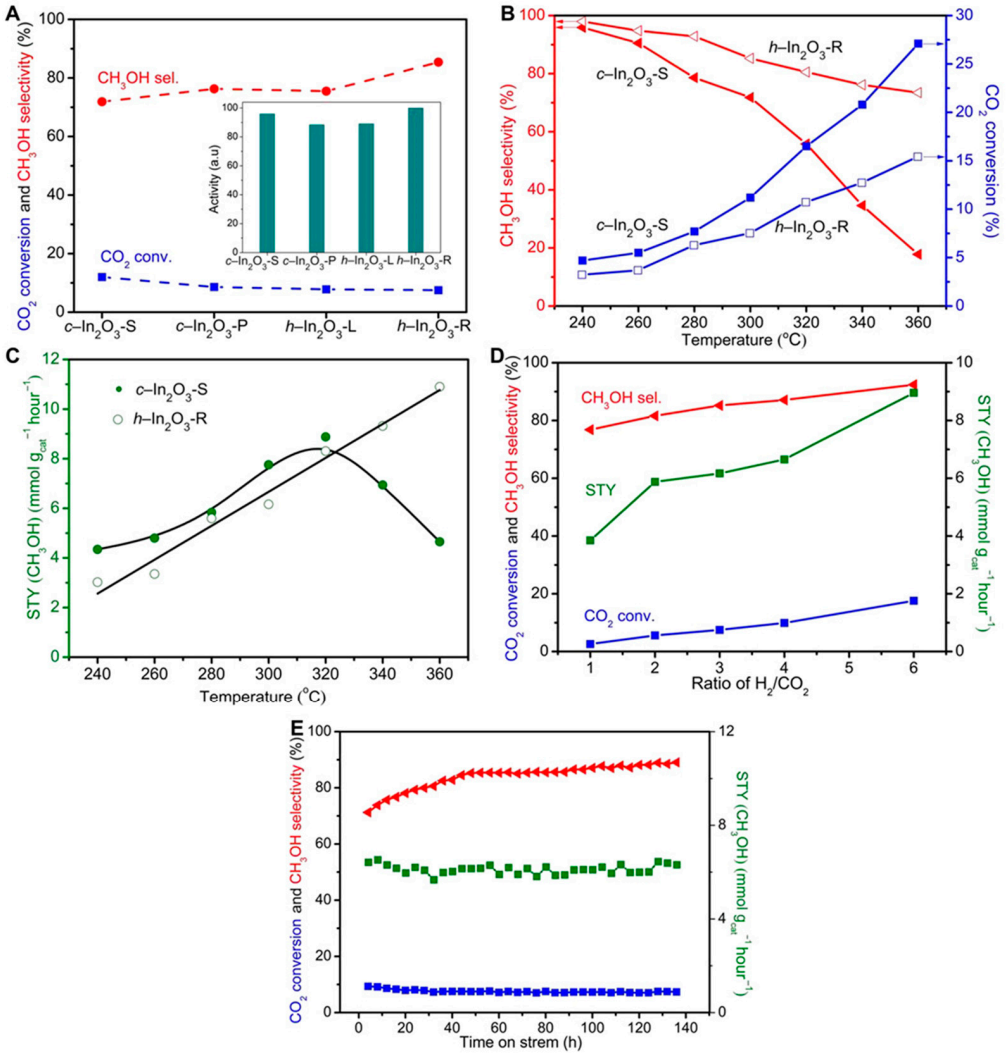

Figure 2. The catalytic activity of different In_2O_3 nanomaterials in CO_2 hydrogenation: (**A**) CO_2 conversion and methanol selectivity over In_2O_3 with different crystal phases and morphologies. (**B**) Effect of temperature on conversion of CO_2 and selectivity of methanol over *c*-In_2O_3-S and *h*-In_2O_3-R. (**C**) Effect of temperature on space-time yield (STY) over *c*-In_2O_3-S and *h*-In_2O_3-R. (**D**) Effect of H_2/CO_2 molar ratio over *h*-In_2O_3-R. (**E**) Catalytic stability of *h*-In_2O_3-R. Reproduced with permission from ref. [63]. Copyright 2020 American Association for the Advancement of Science.

Although In_2O_3 exhibited excellent methanol selectivity in CO_2 hydrogenation, the low CO_2 conversion limited the methanol yield. Therefore, based on the cognition of the In_2O_3 active site and the reaction pathway of CO_2 hydrogenation over In_2O_3, two strategies shown in Figure 4 were adopted to enhance the performance of In_2O_3, including (I) introducing other metal elements into In_2O_3 and (II) combining In_2O_3 with other metal oxides. The catalytic performance of In_2O_3-based catalysts is summarized in Table 1.

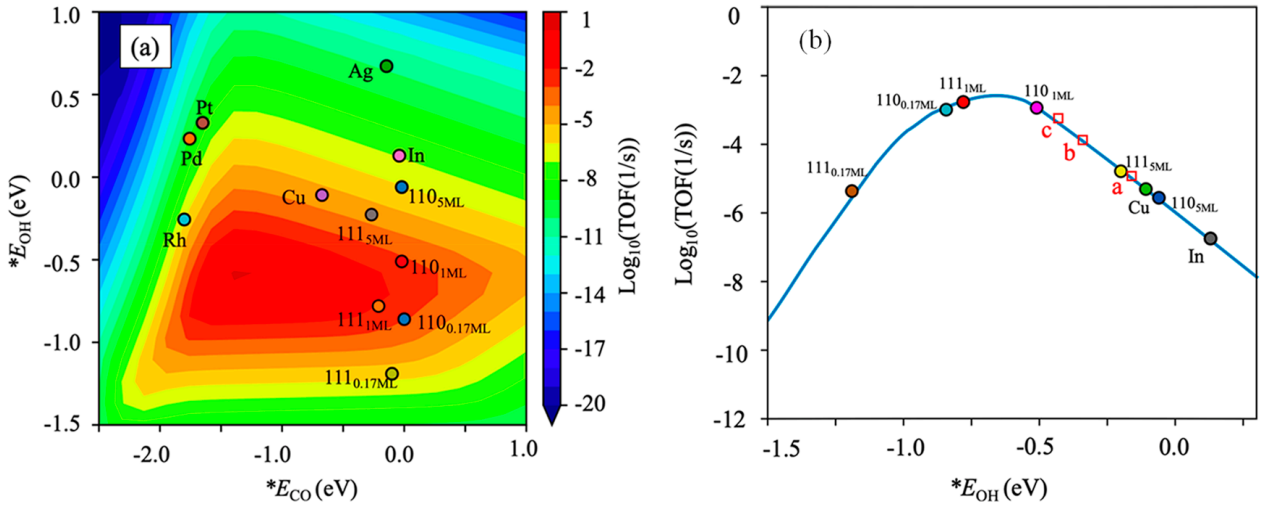

Figure 3. (**a**) Theoretical activity volcano of methanol synthesis from CO_2 hydrogenation over In_2O_3 and transition-metal (211) surfaces. (**b**) The relationship between methanol formation and OH binding energy (fixed CO adsorption energy: −0.1 eV). Reproduced with permission from ref. [65]. Copyright 2021 American Chemical Society.

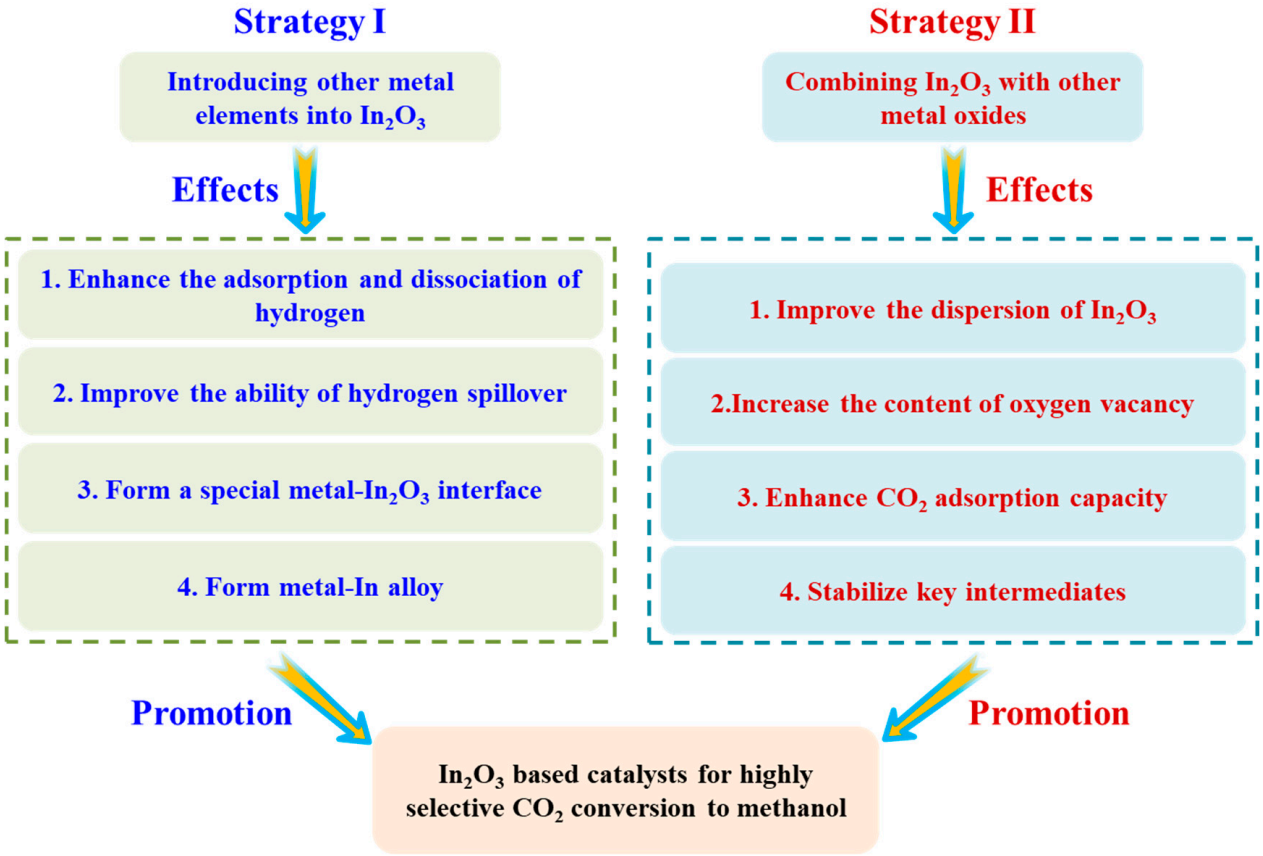

Figure 4. Two representative strategies for improving the performance of In_2O_3.

Table 1. Catalytic performance of In_2O_3-based catalysts in previous study.

Strategies	Catalysts	*P* (MPa)	*T* (°C)	H_2/CO_2 Molar Ratio	CO_2 Conversion (%)	Methanol Selectivity (%)	STY (g_{MeOH} h^{-1} g_{cat}^{-1})	Ref.
Intrinsic activity	In_2O_3	4	330	3:1	7.1	39.7	~0.12	[38]
	In_2O_3	5	300	4:1	[a]	100	~0.18	[58]
	In_2O_3	5	300	4:1	9.4	~62.5	~0.34	[61]
	c-In_2O_3	4	340	4:1	~12.0	~19.0	~0.09	[62]
	rh-In_2O_3	4	340	4:1	~5.0	~30.0	~0.05	[62]
	c-In_2O_3	3	300	3:1	~4.0	~70.5	0.06	[64]
	h-In_2O_3	3	300	3:1	~4.7	~71.0	0.07	[64]
	c/*h*-In_2O_3-1	3	300	3:1	~5.7	~72.3	0.09	[64]
	c/*h*-In_2O_3-2	3	300	3:1	~6.2	~73.0	0.10	[64]
	c/*h*-In_2O_3-3	3	300	3:1	~5.0	~72.1	0.08	[64]
Introducing other metal elements into In_2O_3	Pd-P/In_2O_3	5	300	4:1	~20.0	~70.0	0.89	[68]
	h-In_2O_3/Pd	3	300	3:1	~10.5	72.4	0.53	[69]
	Pd/MnO/In_2O_3	3	280	3:1	4.5	71.3	0.24	[70]
	Pt/In_2O_3	5	300	4:1	17.3	~54.0	0.54	[61]
	Pt/In_2O_3	4	300	3:1	5.7	~71.5	~0.75	[71]
	Rh/In_2O_3	5	300	4:1	17.1	56.1	0.54	[72]
	Rh-5-In_2O_3	5	270	4:1	10.0	71.0	0.52	[73]
	Ru/In_2O_3	5	300	4:1	14.3	69.7	0.57	[74]
	Au/In_2O_3	5	300	4:1	11.7	67.8	0.47	[75]
	Ir/In_2O_3	5	300	4:1	17.7	~70.0	~0.77	[76]
	Ni/In_2O_3	5	300	4:1	18.4	~54.0	0.55	[77]
	Ni/In_2O_3	3	250	3:1	3.0	~52.0	~0.25	[78]
	Co/In_2O_3	4	300	3:1	~9.0	~40.0	~0.31	[79]
	In_2O_3@Co_3O_4	5	250	4:1	8.3	~87.0	0.65	[80]
	$Cu_{11}In_9$-In_2O_3	3	260	3:1	10.3	86.2	~0.19	[81]
Combining In_2O_3 with other metal oxides	In_2O_3/ZrO_2	5	300	4:1	[a]	~100	~0.31	[58]
	In_2O_3/m-ZrO_2	3	280	3:1	12.1	84.6	[a]	[82]
	$In_{2.5}$/ZrO_2	5	280	4:1	[a]	60.0	~0.07	[83]
	$Ga_{0.4}In_{1.6}O_3$	3	320	3:1	~12.0	~28.0	[a]	[84]
	InCe oxides	0.1	290	3:1	[a]	~10.0	~0.12 [b]	[85]
	In_2O_3/Al_2O_3	5	280	4:1	[a]	[a]	~0.04	[86]

[a] Not available. [b] μmol_{MeOH} s^{-1} g_{In}^{-1}.

2.2. Metal/In_2O_3 Composite Catalysts

The abundant oxygen vacancies in In_2O_3 can adsorb and activate CO_2, and the periodic generation and annihilation of oxygen vacancies can inhibit the side reactions, leading to the highly selective conversion of CO_2 to methanol. However, the weak hydrogen adsorption and dissociation of In_2O_3 limit the hydrogenation of carbon species, so CO_2 conversion is very low. Accordingly, the introduction of a noble metal or transition metal (M) could improve CO_2 conversion due to the synergistic catalysis of M and In_2O_3. As shown in Figure 5, the H_2 molecule was adsorbed and activated on the M surface to generate H active species (step ①) and then combined with lattice oxygen of In_2O_3 via spillover (step ②) to create the oxygen vacancies (step ③). CO_2 molecule was adsorbed and activated by the obtained oxygen vacancies (step ④) and finally hydrogenated to methanol by combining with H active species (step ⑤).

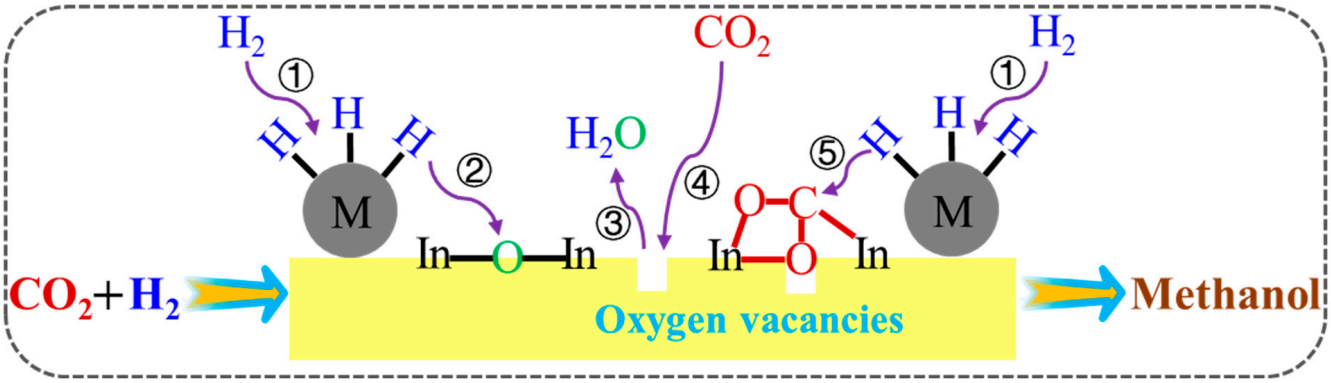

Figure 5. The synergistic catalysis effect of M and In_2O_3 in CO_2 hydrogenation to methanol.

2.2.1. Noble Metal/In_2O_3 Catalysts

Pd/In_2O_3 catalyst. Many investigations have been concentrated on Pd/In_2O_3 catalyst for CO_2 hydrogenation to methanol in recent years. Ge et al. [87] studied methanol synthesis from CO_2 hydrogenation over Pd/In_2O_3 by the DFT method. They found that the HCOO* route competes with the RWGS route over Pd/In_2O_3 in the reaction process, and $H_2COO^* + H^* \leftrightarrows H_2CO^* + OH^*$ and $cis\text{-}COOH^* + H^* \leftrightarrows CO^* + H_2O^*$ were their rate-limiting steps, respectively. The HCOO* route was the major pathway for methanol synthesis from CO_2 hydrogenation. Moreover, the H adatom activated by the Pd cluster and H_2O on the In_2O_3 substrate was extremely significant for the promotion of methanol production, and the adsorbed hydroxyl on the interface of Pd/In_2O_3 can induce the transformation of the Pd_4 cluster, which caused the change in final hydrogenation step. According to the guidance of the theoretical study, they prepared Pd/In_2O_3 with high dispersion of Pd nanoparticles by thermal treatment of Pd-peptide composite/In_2O_3 for methanol synthesis from CO_2 hydrogenation [68]. The prepared catalyst exhibited much more excellent activity than that of pure In_2O_3 due to the better ability to adsorb and dissociate H_2 for hydrogenation steps and the formation of oxygen vacancies. As a result, such a catalyst was able to demonstrate 20% of CO_2 conversion, 70% of methanol selectivity, and 0.89 $g_{MeOH}\ h^{-1}\ g_{cat}{}^{-1}$ of space-time yield (STY), respectively.

Huang et al. [69] from our group detailly investigated the effect of strong metal–support interaction between Pd and In_2O_3 on the catalytic performance of CO_2 hydrogenation to methanol by adjusting the morphology of In_2O_3. The results indicated that the combination of Pd and hollow In_2O_3 nanotubes derived from MIL-68(In) nanorod was more conducive to the methanol production compared with other morphologies of In_2O_3, which was due to more formation of Pd^{2+} via electron transfer from Pd to the curved In_2O_3 (222) to enhance H_2 adsorption and formation of surface oxygen vacancies. In addition, to prevent the formation of the In-Pd bimetallic phase that led to the quick deactivation of the catalyst, our group further developed TCPP(Pd)@MIL-68(In) as precursors to prepare Pd/In_2O_3 [88]. Compared to $PdCl_2$, TCPP(Pd) (metalloporphyrins) can be served as a capping agent for the growth of MIL-68(In) and a shuttle for transporting the Pd^{2+}, thereby improving the dispersion of Pd during the process of calcination and reduction, and preventing excessive reduction to form In-Pd bimetallic phase. Both theoretical and experimental results indicated that the prepared Pd/In_2O_3 possessed excellent thermodynamic selectivity for methanol. For the same purpose of reducing the formation of In-Pd alloy, Zhan et al. [89] from our group adopted rape pollen pretreated by hydrochloric acid as the biological template to fabricate hierarchically structured bio-In_2O_3 and bio-In_2O_3/Pd, as shown in Figure 6. The results suggested that the pollen template with acid etching possessed a hollow cage-like structure and abundant functional groups (viz., -COOH and -NH_2) on the surface, which was conducive to the growth of In_2O_3 with abundant superficial oxygen vacancies. Compared to the sample without acid pretreatment (bio-In_2O_3-0/Pd), bio-In_2O_3-15/Pd demonstrated a better ability to inhibit the formation of In-Pd alloy due to the more

uniform In_2O_3 spatial distribution to reduce the interaction between Pd and In_2O_3. In the following research, our group further developed bifunctional catalyst Pd/In_2O_3/H-ZSM-5 for dimethyl ether synthesis from CO_2 hydrogenation, whereby Pd/In_2O_3 prepared by carbonized alginate templating favored CO_2 hydrogenation into methanol, and H-ZSM-5 favored methanol dehydration into dimethyl ether. Compared to commercial Pd/In_2O_3 (Com-PdIn), microspherical-confined nano In_2O_3 possessed more excellent texture properties to disperse the Pd nanoparticles, thus obtaining more than 450 g_{MeOH} kg_{cat}^{-1} h^{-1} of STY, whereas Com-PdIn only achieved 50.8450 g_{MeOH} kg_{cat}^{-1} h^{-1} of STY [90].

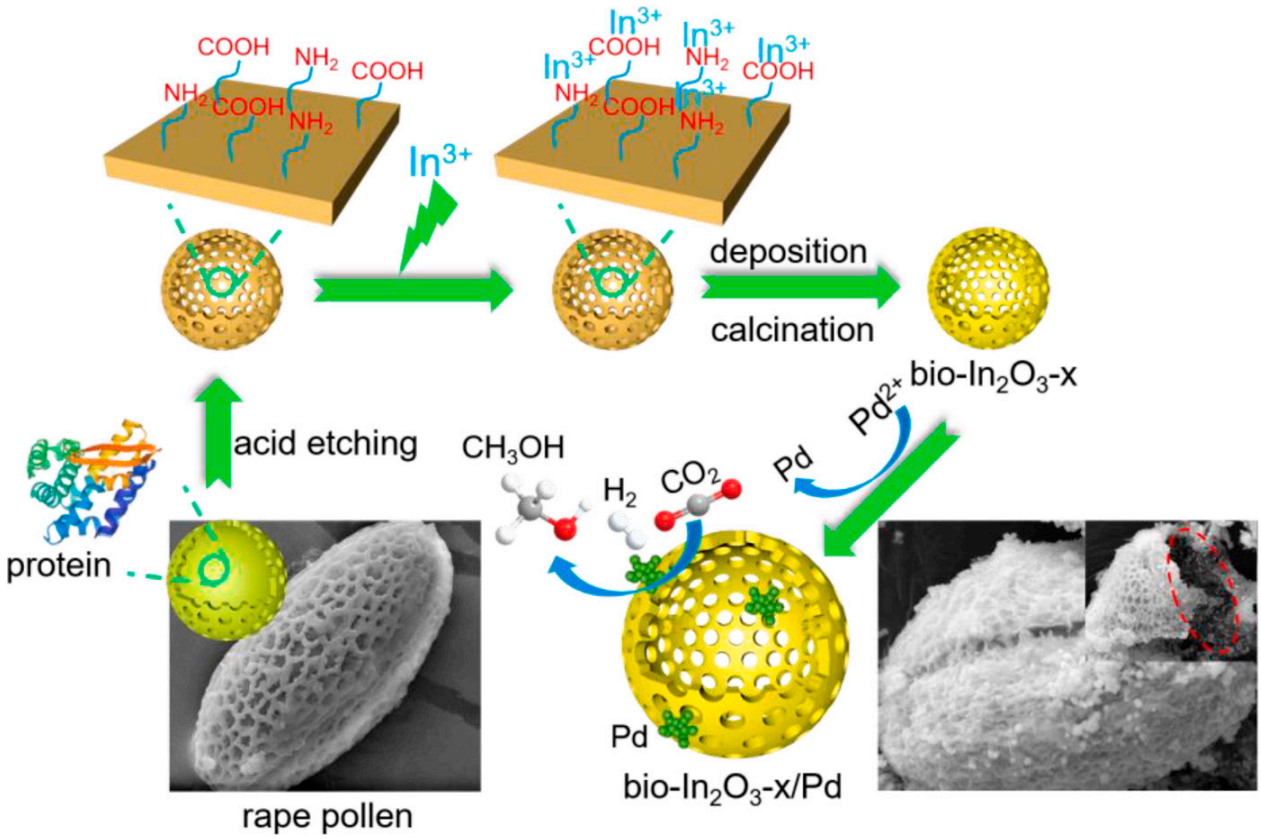

Figure 6. Fabrication routes of supported bio-In_2O_{3-x}/Pd catalysts. Reproduced with permission from ref. [89]. Copyright 2021 Elsevier.

Pérez-Ramírez et al. [91] reported an effective coprecipitation method to incorporate isolated palladium atoms into an In_2O_3 lattice for forming low-nuclearity palladium clusters, which can overcome the selectivity and stability limitations associated with palladium nanoparticles. Additionally, to disperse the active components highly, Zhang et al. [92] employed the citric acid method to load In_2O_3 and Pd on SBA-15, respectively. It can be found that oxygen vacancies were promoted with increasing Pd amount. The as-prepared catalyst possessed excellent performance with 12.9% of CO_2 conversion, 83.9% of methanol selectivity, and 1.1×10^{-2} mol_{MeOH} h^{-1} g_{cat}^{-1} of STY, which was due to the high dispersion of In_2O_3 and Pd nanoparticles on SBA-15, and the synergetic effect of H_2 dissociation on Pd species and CO_2 activation on In_2O_3. Moreover, Wu et al. [70] introduced Mn and Pd into In_2O_3 to improve the methanol selectivity and CO_2 conversion. The results showed that Pd species were highly dispersed on the MnO/In_2O_3 due to the strong metal–support interactions, and 1 wt% $Pd/MnO/In_2O_3$ exhibited excellent activity (240.6 g_{MeOH} kg_{cat}^{-1} h^{-1} of STY) and stability in CO_2 hydrogenation.

Pt/In_2O_3 catalyst. The combination of Pt and In_2O_3 for CO_2 hydrogenation to methanol has also been reported. For instance, Li et al. [71] adopted the coprecipitation method to synthesize Pt/In_2O_3 and investigated the effect of Pt content on the catalytic performance.

They found that as Pt content increased, CO_2 conversion increased, whereas methanol selectivity increased first and then decreased. The highly dispersed Pt^{n+} was embedded into the In_2O_3 lattice to promote the formation of oxygen vacancies and contribute to CO_2 activation. In the reaction process, the unstable Pt^{n+} was reduced to Pt nanoparticle, and the stable Pt^{n+} kept the high dispersion. Both Pt^{n+} and Pt can activate H_2, but the effect on the reaction was quite different; specifically, the highly dispersed Pt^{n+} was used as the Lewis acid site to promote H_2 dissociation for CO_2 hydrogenation to methanol, while Pt nanoparticles induced the RWGS reaction to decrease the methanol selectivity. Similarly, Liu et al. [61] supported Pt on In_2O_3 to improve the methanol yield. The results showed that the CO_2 conversion and methanol yield over Pt/In_2O_3 were 17.3% and 0.542 g_{MeOH} h^{-1} $g_{cat}{}^{-1}$ at 300 °C, respectively (In_2O_3: 9.4% and 0.335 g_{MeOH} h^{-1} $g_{cat}{}^{-1}$). As compared to In_2O_3, Pt/In_2O_3 possessed more excellent catalytic stability, which was mainly due to the high dispersion of Pt nanoparticles and strong interaction between Pt and In_2O_3 to inhibit the excessive reduction in In_2O_3. In addition, to keep the high dispersion of Pt, Pan et al. [93] synthesized $Pt/film/In_2O_3$ catalyst shown in Figure 7 via the cold-plasma/peptide-assembly (CPPA) method. The prepared $Pt/film/In_2O_3$ obtained 37.0% of CO_2 conversion and 62.6% of methanol selectivity at 30 °C and 0.1 MPa in a dielectric barrier discharge (DBD) plasma reactor. The film of the catalyst played significant roles in the improvement of catalytic performance, namely inhibiting the agglomeration of Pt nanoparticles and transferring the electrons from the catalyst to CO_2. The results of this work provided a valuable reference for CO_2 hydrogenation to methanol at room temperature and pressure. Pérez-Ramírez et al. [94] highlighted flame spray pyrolysis as a synthesis platform to assess metal (Pt, Ni, Au, etc.) promotion in In_2O_3-based catalysts for CO_2 hydrogenation. Compared to Ni clusters or Au nanoparticles, the atomically dispersed and well-stabilized Pt had a more obvious promoting effect on In_2O_3 for CO_2 hydrogenation to methanol. Moreover, DFT simulations further revealed that the high concentration of isolated Pt atoms could greatly enhance homolytic H_2 splitting and increase the availability of hydrides for C-H hydrogenation due to the formation In_3Pt and In_2Pt_2 ensembles, therefore facilitating methanol production.

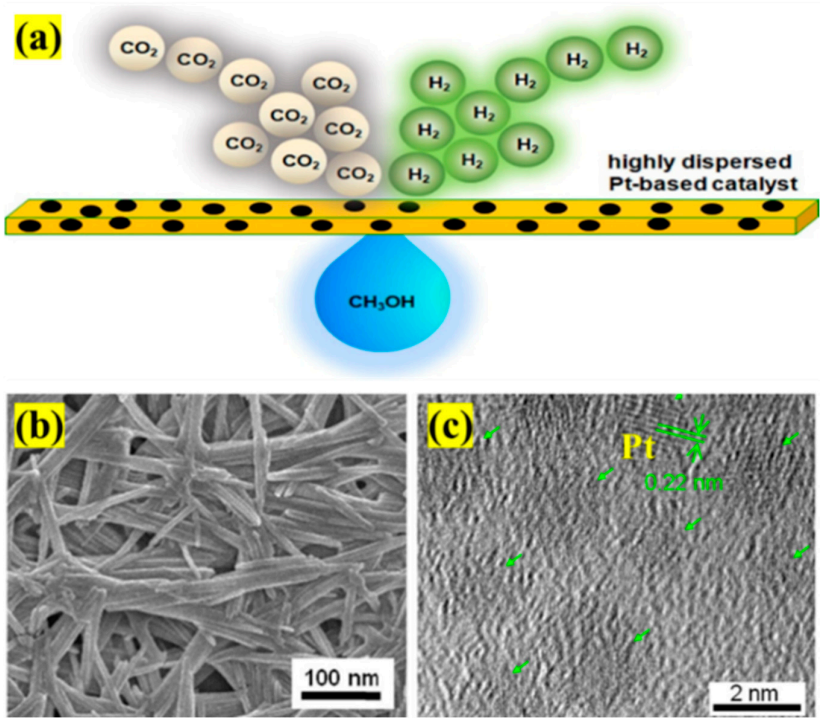

Figure 7. (**a**) The structure model of $Pt/film/In_2O_3$. (**b**) SEM image of $Pt/film/In_2O_3$. (**c**) HRTEM image of $Pt/film/In_2O_3$. Reproduced with permission from ref. [93]. Copyright 2019 Elsevier.

Other noble metal/In_2O_3 catalyst. In addition to Pd and Pt, other noble metals were also introduced into In_2O_3 to promote catalytic performance. Shrotri et al. [73] found that methanol STY over In_2O_3-based catalyst can be improved from 0.18 g_{MeOH} h^{-1} $g_{cat}{}^{-1}$ to 1.0 g_{MeOH} h^{-1} $g_{cat}{}^{-1}$ after doping of Rh. This was because, on the one hand, Rh promoted the dissociation of H_2 to lead to the formation of more oxygen vacancies on the In_2O_3 surface. On the other hand, Rh was related to the production of formate species with a low activation barrier confirmed by DFT. Similarly, Liu et al. [72] also investigated the influence of Rh addition to In_2O_3 on methanol production from CO_2 hydrogenation. They demonstrated that the existence of Rh can enhance the dissociative adsorption and spillover of hydrogen, which was instrumental in surface oxygen vacancies formation of In_2O_3 and CO_2 activation, so the STY of 0.5448 g_{MeOH} h^{-1} $g_{cat}{}^{-1}$ over Rh/In_2O_3 was obtained while it was only 0.3402 g_{MeOH} h^{-1} $g_{cat}{}^{-1}$ over In_2O_3. In addition, they also supported Ru [74], Au [75], Ir [76], and Ag [95] on the In_2O_3 for CO_2 hydrogenation to methanol, and the results indicated that the catalytic activity could be enhanced to a great extent.

2.2.2. Base Metal/In_2O_3 Catalysts

Ni/In_2O_3 catalysts. Recently, Ni/In_2O_3 catalysts have also attracted wide attention in methanol production from CO_2 hydrogenation. In 2020, Liu et al. [77] prepared an In_2O_3-supported nickel catalyst (Ni/In_2O_3) by a wet chemical reduction for CO_2 hydrogenation, and the results suggested that the highly dispersed Ni species can be used as active sites for hydrogen dissociation and spillover to contribute to the formation of oxygen vacancies and hydrogenation process. Therefore, the effective synergy of Ni sites and In_2O_3 support resulted in superior catalytic performance, specifically, 18.47% of CO_2 conversion, more than 54% of methanol selectivity, and 0.55 g_{MeOH} h^{-1} $g_{cat}{}^{-1}$ of STY at 300 °C and 5 MPa. Subsequently, to further understand the superior catalytic performance of Ni/In_2O_3, they investigated the synergistic effect of the metal–support interaction and interfacial oxygen vacancies on methanol synthesis via DFT calculation [96]. It was found that the interfacial oxygen vacancies were beneficial for boosting the CO_2 adsorption and charge transfer between the nickel species and indium oxide, synergistically promoting the selectivity of methanol. Simultaneously, among the three reaction pathways examined (formate pathway, CO hydrogenation, and RWGS pathway, respectively), the RWGS pathway was proven to be the most theoretically favored for methanol synthesis from CO_2 hydrogenation over Ni/In_2O_3, as shown in Figure 8. In addition to the above research work, they also introduced ZrO_2 into Ni/In_2O_3 catalyst (Ni/In_2O_3-ZrO_2) for CO_2 hydrogenation to methanol [97]. The solid solution formed by ZrO_2 and In_2O_3 can optimize and stabilize the oxygen vacancies of In_2O_3 to avoid the excessive reduction in the bulk indium oxide, thus possessing a 43.2% increase in STY of methanol. Different from the traditional synthesis method, Hensen et al. [78] combined Ni with In_2O_3 using flame spray pyrolysis (FSP) synthesis. The obtained NiO-In_2O_3 catalyst possesses high specific surface areas and block morphology. When NiO loading is 6 wt%, ~0.25 g_{MeOH} h^{-1} $g_{cat}{}^{-1}$ of STY can be obtained over the corresponding catalyst at the conditions of 250 °C and 30 bar. The comprehensive characterizations revealed the strong interactions between Ni cations and In_2O_3 when NiO loading is lower 6 wt%, which contributed to the promotion of surface density of oxygen vacancies. Additionally, DFT calculation suggested that the introduction of Ni species lowered the energy barrier of H_2 dissociation to facilitate hydrogenation of adsorbed CO_2 on oxygen vacancies.

Other metal/In_2O_3 catalysts. To improve the performance of In_2O_3, Qi et al. [79] prepared In_x-Co_y oxides catalysts for CO_2 hydrogenation to methanol. It was found that the methanation activity catalyzed by Co species was suppressed, and the best catalyst (In_1-Co_4) exhibited nearly five times methanol STY compared to that of pure In_2O_3 at conditions of 300 °C and 4 MPa. Several in situ and ex situ characterizations suggested that CO_2 hydrogenation over Co species and In_x-Co_y oxides all followed the formate pathway, and much stronger adsorbed capacity of CO_2 and carbon-containing intermediates on In_x-Co_y oxides catalyst contributed to a feasible surface C/H ratio, therefore facilitating CH_3O*

to produce methanol instead of being over-hydrogenated to methane. Gascon et al. [80] explored metal–organic framework (MOF) mediated synthetic approaches to prepare a Co_3O_4-supported In_2O_3 catalyst for CO_2 hydrogenation to methanol. Compared to the traditionally coprecipitated In@Co catalytic system, the induction period in the hydrogenation process over MOF-derived In@Co catalyst could be tuned because ZIF-67(Co) support provided better In dopant distribution. In addition, the sequential pyrolysis-calcination steps could promote the formation of mixed-metal carbide ($Co_3InC_{0.75}$) to stabilize high In distribution and prevent the formation of large individual oxide domains, thus leading to a faster induction period. The prepared catalyst (used 3In@8Co(300)) showed nanoparticles featuring core–shell morphologies (Co-In oxides shell over $Co_3InC_{0.75}$ core) shown in Figure 9 and could obtain 0.65 g_{MeOH} h^{-1} $g_{cat}{}^{-1}$ of maximum STY with methanol selectivity of 87% at conditions of 250 °C and 50 bar. Additionally, based on ZIF-67(Co), Zhang et al. [98] obtained a Co/C-N catalyst through the pyrolysis method and then mixed it with In_2O_3 in different methods to prepare In_2O_3/Co/C-N for CO_2 hydrogenation to methanol. It was found that the proximity of Co/C-N and In_2O_3 played a significant role in the synergetic catalysis for methanol synthesis from CO_2 hydrogenation. Moreover, the obvious difference in placement of separate Co/C-N and In_2O_3 in catalytic performance also indicated CO_2 might be adsorbed and activated on the surface of In_2O_3 to form carbon intermediates and then were further hydrogenated into methanol or byproducts over Co/C-N surface. Furthermore, the existence of the N element could improve the electron interaction of Co and In_2O_3 and prevent the sintering of In_2O_3 particles, thereby increasing the catalytic activity and stability for CO_2 hydrogenation to methanol.

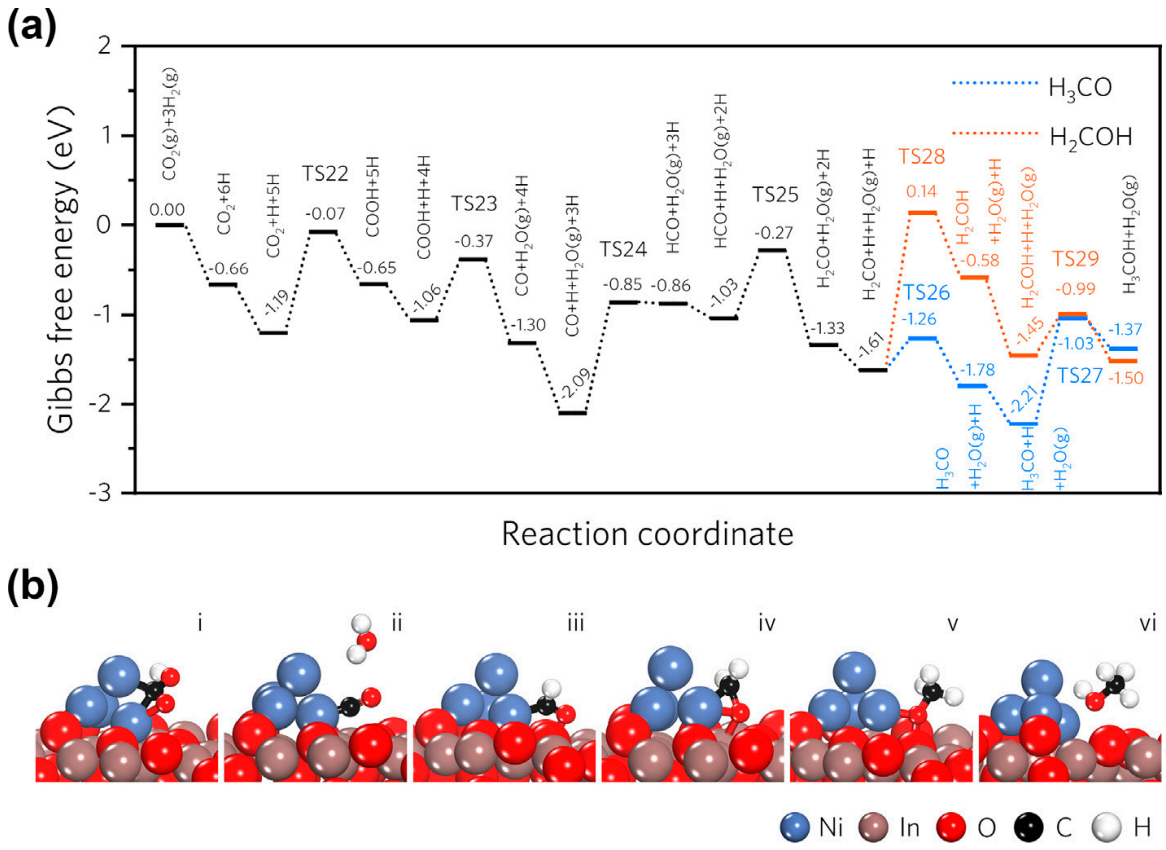

Figure 8. Catalytic mechanism investigation of methanol synthesis via RWGS pathway over Ni_4/In_2O_3 catalyst: (**a**) calculated Gibbs free energy profile; (**b**) surface configurations of Ni_4/In_2O_3_D model at each elementary step. Reproduced with permission from ref. [96]. Copyright 2019 Elsevier.

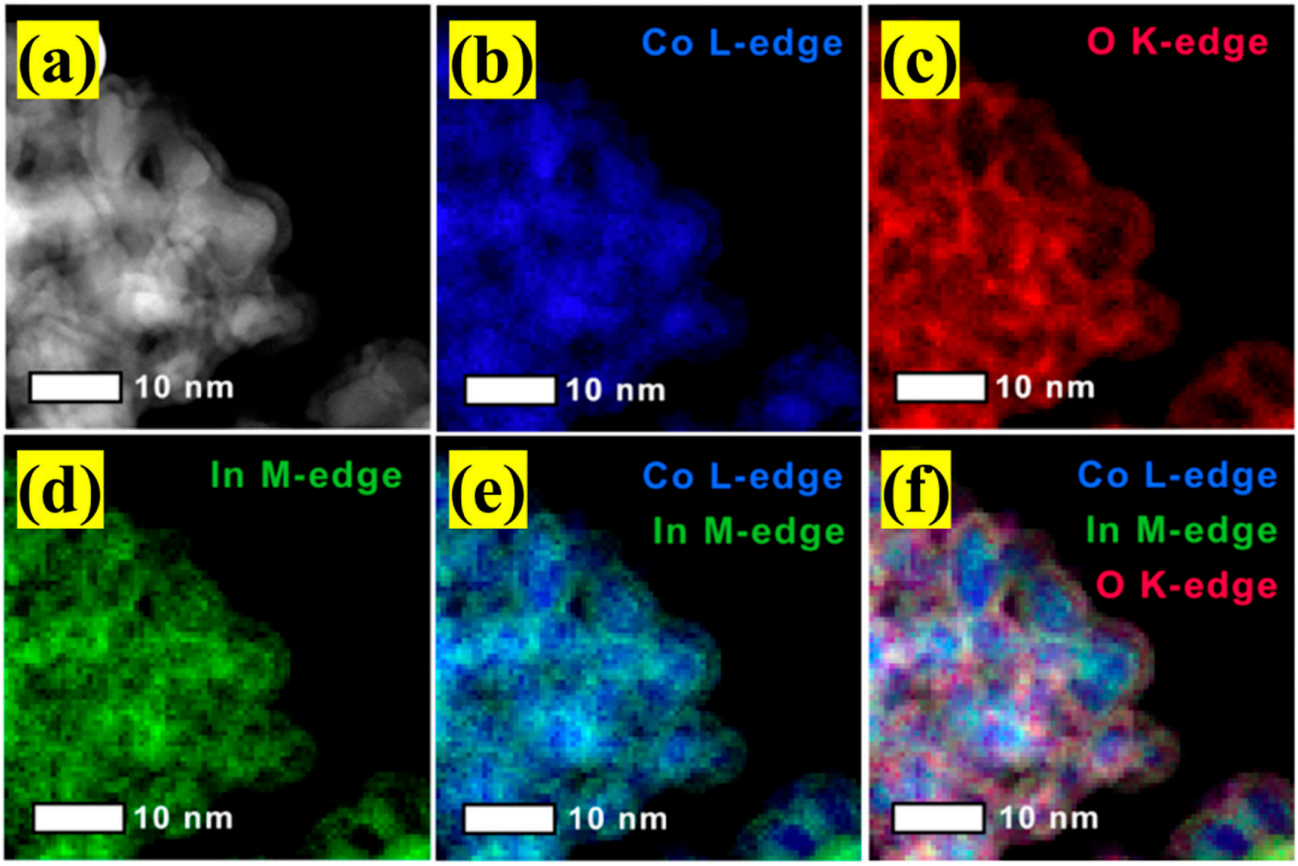

Figure 9. ADF-STEM imaging and elemental mapping for used 3In@8Co(300): (**a**) ADF-STEM image, (**b**) Co map, (**c**) O map, (**d**) In map, (**e**) superimposed Co/In maps, and (**f**) superimposed Co/In/O maps. Reproduced with permission from ref. [80]. Copyright 2020 American Chemical Society.

Additionally, the combination of Cu and In_2O_3 also can be a good choice to improve the catalytic performance. Wu et al. [81] employed the coprecipitation method to fabricate various CuO-In_2O_3 and investigated the effect of the Cu:In molar ratio on the physicochemical properties and catalytic activity for methanol synthesis. The prepared catalyst mainly exhibited in the form of $Cu_{11}In_9$ phase and In_2O_3 at low Cu:In molar ratio ($\leq$1:2) after reduction treatment or in the reaction process, whereas with the increase in Cu content, Cu_7In_3 phase was continuously weakened, and Cu phase emerged, which resulted in the formation of Cu-Cu_7In_3-In_2O_3. CuIn(1:2) catalyst obtained maximum methanol STY (5.95 $mmol_{MeOH}$ h^{-1} g^{-1}) at the conditions of 260 °C and 3.0 MPa due to the highest Cu dispersion and the highest surface oxygen vacancies concentration, and the synergistic effect, Cu_7In_3 phase for H_2 dissociation and In_2O_3 for CO_2 adsorption, were considered as the major contributions for the efficient catalytic efficiency. The interfacial sites between Cu and metal oxides (In, Zn, and Zr) were tuned by Yu et al. for CO_2 hydrogenation to methanol [99]. The results suggested that the introduction of In_2O_3 into Cu/ZrO_2 catalyst can increase the methanol formation rate from 52.7 mmol $g_{cat}{}^{-1}$ to 60.5 mmol $g_{cat}{}^{-1}$. This was because, on the one hand, the formation of Cu_xIn_y surface species inhibited the RWGS reaction on the Cu surface. On the other hand, ZrO_2 stabilized the In_2O_3 and generated additional In-Zr mixed oxide sites for CO_2 conversion to methanol.

2.3. In_2O_3/Metal Oxides Composite Catalysts

Combining In_2O_3 with other metal oxides is also a significant strategy, which can improve the dispersion of In_2O_3, increase the content of oxygen vacancies for CO_2 adsorption, and stabilize the key intermediates to facilitate methanol formation from CO_2 hydrogenation. Supporting In_2O_3 on ZrO_2 is the most common and effective method

because the electronic structure effect and crystal lattice mismatching between In_2O_3 and ZrO_2 are beneficial to CO_2 activation for the formation of methanol. The research results by Pérez-Ramírez et al. proved that combining In_2O_3 with ZrO_2 can enhance the catalytic activity and stability of CO_2 hydrogenation to methanol [58]. On the one hand, the reduced Zr centers can attract oxygen atoms from the active phase in the reaction process, therefore increasing oxygen vacancies for CO_2 adsorption and activation. On the other hand, ZrO_2 support effectively improved the dispersion of In_2O_3 nanoparticles. Next, they explored the electronic, geometric, and interfacial phenomena between In_2O_3 and ZrO_2 [86]. The results suggested that the catalytic performance of mixed In-Zr oxides could not be improved by coprecipitation, thereby excluding the primary role of electronic parameters. The epitaxial growth of In_2O_3 was permitted on both monoclinic and tetragonal ZrO_2; however, the more obvious lattice mismatching contributes to the lower dispersion of In_2O_3 on monoclinic ZrO_2. Detailed characterizations and kinetic analyses revealed two major facilitation of monoclinic ZrO_2 support for In_2O_3 performance. One is that the epitaxial alignment of In_2O_3 on monoclinic ZrO_2 ensured the high dispersion of the oxide to prevent sintering. The other is that the less favorable lattice matching between In_2O_3 and monoclinic ZrO_2 produces tensile strain more easily, favoring the formation of oxygen vacancies on In_2O_3. The strong electronic oxide–support interaction between In_2O_3 and ZrO_2 for CO_2 hydrogenation to methanol was investigated by Gong et al. through quasi-in situ XPS experiments and DFT calculation [82]. Compared to the combination of In_2O_3 and tetragonal ZrO_2 (In_2O_3/t-ZrO_2), In_2O_3/m-ZrO_2 (m-: monoclinic) exhibits more excellent catalytic performance (CO_2 conversion up to 12.1% with methanol selectivity of 84.6%) due to the stronger interaction to lead to the high dispersion of In-O-In over m-ZrO_2. Methanol synthesis from CO_2 hydrogenation over In_2O_3/m-ZrO_2 follows the formate pathway. It was confirmed that the electron was transferred from m-ZrO_2 to In_2O_3 to generate electron-rich In_2O_3, which can facilitate the dissociation of H_2 and help HCOO* transform into CH_3O* by hydrogenation. Blum et al. [100] paid important attention to the support effect and surface reconstruction of In_2O_3/m-ZrO_2 in the process of CO_2 hydrogenation to methanol. They proposed that the modifying effects of m-ZrO_2 on In_2O_3 mainly had two aspects: (I) m-ZrO_2 serves as a reservoir for partially reduced In_2O_3 (InO_x, $0 < x < 1.5$) due to the fact that InO_x can semireversibly migrate in and out of the subsurface of m-ZrO_2 under reaction conditions (623 K). The decrease in surface InO_x concentration at high temperatures resulted in the low selectivity toward methanol and a rapid increase in RWGS reaction. (II) The interaction that Zr centers attracted the O atom of In_2O_3 led to the activation of the In-O bond at the In_2O_3-m-ZrO_2 interface to generate oxygen vacancies, and the high dispersion of In_2O_3 nanoparticles on m-ZrO_2 prevented the over-reduction of In_2O_3 under catalytic conditions compared to the bare In_2O_3. Based on their work, they also summarized the reaction mechanism pathway on the bare In_2O_3 and In_2O_3/m-ZrO_2, as exhibited in Figure 10. Witoon et al. [101] studied the effect of the calcination temperature of ZrO_2 support on the physicochemical properties and catalytic activities of In_2O_3/ZrO_2 for converting CO_2 and H_2 into methanol at a high reaction temperature. As the calcination temperature increased (from 600 to 1000 °C), the crystal of ZrO_2 support gradually changed from an amorphous phase to a tetragonal phase. The high calcination temperature of ZrO_2 support can decrease the reduction degree of In_2O_3, indicating the better interaction between In_2O_3 and tetragonal ZrO_2 compared to amorphous ZrO_2. In addition, the adsorption capacity of prepared In_2O_3/ZrO_2 catalysts for CO_2 and H_2 was enhanced with the increase in calcination temperature of ZrO_2 support, which promoted the highly selective conversion of CO_2 and H_2 into methanol instead of methane, whereas it did not have a significant impact on the formation of CO.

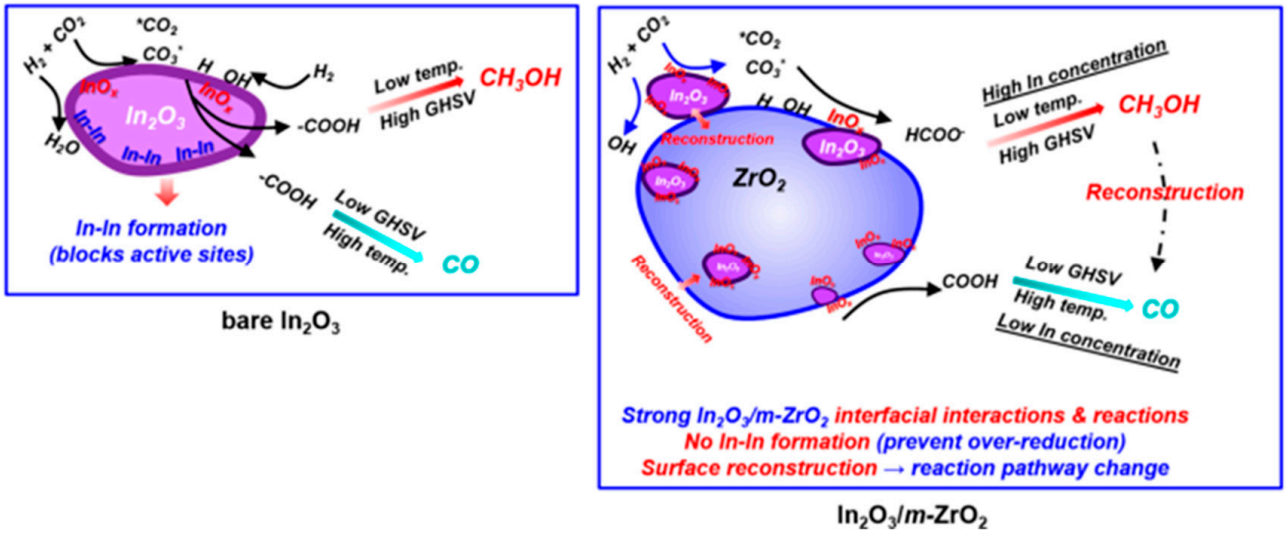

Figure 10. Reaction mechanism pathway on bare In_2O_3 and different In_2O_3/m-ZrO_2 catalysts. Reproduced with permission from ref. [100]. Copyright 2022 American Chemical Society.

Müller et al. [102] investigated the effect of the ZrO_2 phase on the reducibility, local structure, and catalytic performance of In_2O_3/ZrO_2 for CO_2 hydrogenation to methanol by operando X-ray absorption spectroscopy (XAS) and XRD studies. The results suggested that the amorphous ZrO_2 (am-ZrO_2) support could not form a solid solution with In_2O_3, and led to the rapid reduction in In_2O_3 to pure In^0 under reaction conditions, therefore suffering deactivation within minutes. For tetragonal ZrO_2 (t-ZrO_2) support, although it can inhibit the complete reduction of In_2O_3 into In^0, the reduction extent was still too great (an average oxidation state of In below +2), resulting in poor catalytic activity. Surprisingly, it was found that the interaction between In_2O_3 nanoparticles and monoclinic ZrO_2 (m-ZrO_2) can impel atomical dispersion of In^{2+}/In^{3+} into m-ZrO_2 lattice to form solid solution m-ZrO_2:In, which prevented the over-reduction of In species (an average oxidation state of +2.3) and stabilized the active In-oxygen vacancy (V_o)-Zr sites to facilitate CO_2 conversion into methanol. Additionally, the In-V_o-Zr sites were vitally more stable toward reduction than In-V_o-In sites in bixbyite-type In_2O_3, thus exhibiting superior catalytic activity and stability for CO_2 hydrogenation to methanol. Subsequently, they further studied the nature and abundance of sites for the hydrogen dissociation on In_2O_3/ZrO_2-supported catalysts (In_2O_3/m-ZrO_2, In_2O_3/t-ZrO_2, In_2O_3/am-ZrO_2 and m-ZrO_2:In catalysts) in CO_2 hydrogenation to methanol [103]. The results showed that indium hydride species (In-H) and hydroxyl groups (O-H) could be found on the surface of all redox-pretreated catalysts at room temperature when they were exposed to hydrogen, and only a low concentration of hydrogen dissociation sites still existed on the surface of In_2O_3/m-ZrO_2 and m-ZrO_2:In without redox pretreatment. In_2O_3/m-$ZrO_{2(redox)}$ possessed the highest concentration of surface indium sites for heterolytic activation of H_2, and the obtained In-H species can react with CO_2 to form surface formate species (methanol intermediates) at room temperature, indicating the appreciable reactivity of In-H and carbonates on the m-ZrO_2 support. Additionally, the reduction in hydrogen at 400 °C led to the high dispersion of In into m-ZrO_2 to form a m-ZrO_2:In solid solution. Hydrogen dissociation in m-ZrO_2:In solid solution proceeded on In^{3+}-O-Zr^{4+} sites, obtaining In-H and Zr-OH species.

The preparation method of In_2O_3/ZrO_2 also vitally affects the electronic structure effect, thus to optimize the interaction of In_2O_3 and ZrO_2, and the surface exposure degree of In_2O_3, four different compositing strategies (liquid-phase coprecipitation, precipitation-coating method, ball milling method, and incipient wetness impregnation, respectively) for the synthesis of In_2O_3/ZrO_2 were compared by Gao et al. [104]. It was found that the exposure area of In_2O_3 prepared by the precipitation-coating method was the highest (S_{In} = 6.22 m^2 g^{-1}), whereas it was lowest (S_{In} = 1.56 m^2 g^{-1}) by the coprecipitation

method due to the formation of In_2O_3 bulk dispersion with ZrO_2. The dispersion of In_2O_3 on ZrO_2 can inhibit the over-reduction of In_2O_3, and the exposure area of In_2O_3 was beneficial for CO_2 adsorption and activation. Furthermore, DRIFTS results and DFT calculation demonstrated that the oxygen vacancy defects of In_2O_3/ZrO_2 would stabilize the key formate intermediates to facilitate the formation of methanol obeying the carbonate–formate–methoxy pathway, as shown in Figure 11: H_2 was adsorbed on the exposed In_2O_3 surface (H*), and subsequently generated In-H* and O-H* by hydrogen heterolysis. CO_2 was adsorbed and activated by In-V_o-Zr oxygen vacancies to form carbonate species (CO_2*), and then it combined with the activated In-H* to generate the formate intermediate (HCOO*). Later, HCOO* was further hydrogenated into CH_3OH via the pathway of HCOO*→H_2CO*→H_3CO*→CH_3OH. Apart from ZrO_2, Ga_2O_3 [84], CeO_2 [105], and MnO [106] were also used to combine with In_2O_3 for converting CO_2 into methanol, and their promotion for In_2O_3 performance was also associated with the In_2O_3 dispersion, metal–support interactions, or tuning of basic sites.

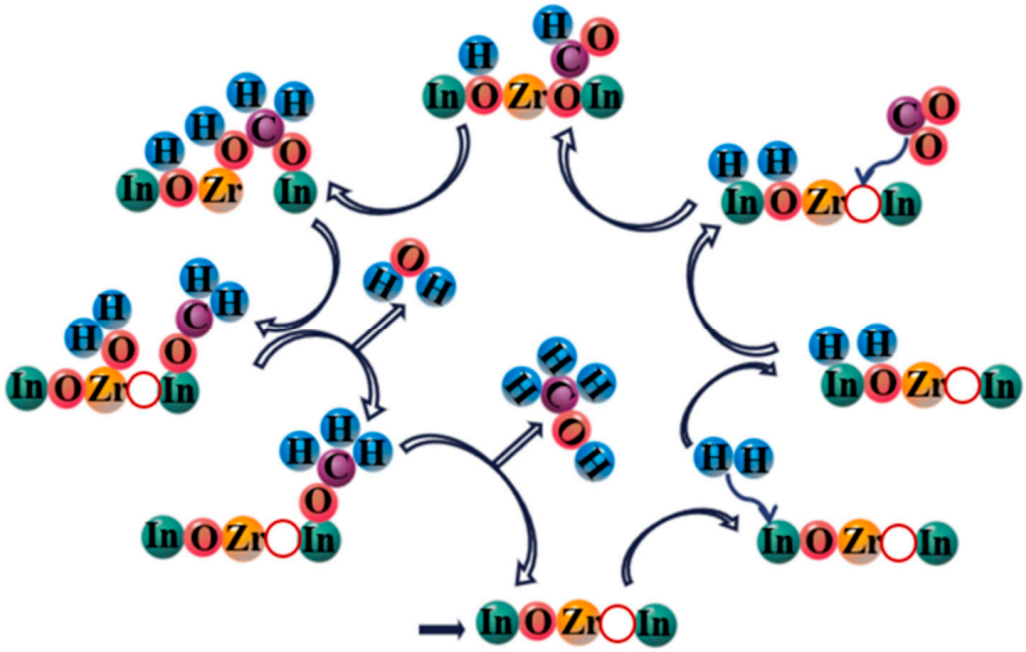

Figure 11. Catalytic mechanism diagram for CO_2 hydrogenation to methanol over In_2O_3/ZrO_2 catalyst prepared by precipitation-coating method. Reproduced with permission from ref. [104]. Copyright 2022 Elsevier.

3. Conclusions and Further Directions

In summary, In_2O_3-based catalysts are promising for the industrial application of thermochemical CO_2 hydrogenation to methanol. Various research methods have been adopted to explore the formation process and possible structure of active sites and the reaction mechanism over In_2O_3-based catalysts for CO_2 hydrogenation to methanol. Furthermore, research has been ongoing to further understand the structure–activity relationship and identify the key factors affecting the catalytic performance. It is commonly accepted that methanol synthesis from CO_2 hydrogenation over In_2O_3-based catalysts follows a formate pathway, where CO_2 adsorbed on the oxygen vacancy of In_2O_3 passes through the route of CO_2*→HCOO*→H_2CO*→H_3CO*→CH_3OH. The phase state of In_2O_3 plays a key role in determining CO_2 conversion and methanol selectivity, and compared to cubic bixbyite-type In_2O_3 (*c*-In_2O_3), hexagonal In_2O_3 (*h*-In_2O_3) with a high proportion of the exposed (104) surface exhibited the higher catalytic activity and possessed high stability, which is mainly due to the facile formation of the oxygen vacancies at low coverage and the favorable formation of the hydride adsorbate at the In sites on (104) surface. The factors dictating

performance improvement of In_2O_3-based catalysts include (1) the ability for dissociation and spillover of hydrogen, (2) the number of oxygen vacancies for CO_2 activation, (3) the dispersion of In_2O_3 nanostructures, and (4) the stability of key intermediates. Two different strategies, metal doping and hybrid with other metal oxides, respectively, are utilized to optimize the above factors for enhancing the catalytic performance of In_2O_3-based catalysts. For the facilitation of dissociation and spillover of hydrogen, the most effective strategy is introducing the metal element (M, M = Pd, Pt, Ni or Co, etc.) into In_2O_3. The existence of M nanostructures sharply promotes the dissociative adsorption of hydrogen, therefore being instrumental in enhancing the hydrogenation process and increasing surface oxygen vacancy. On balance, the synergistic catalysis effect of M and In_2O_3 contributes to the high catalytic performance of M/In_2O_3 catalysts. As for the improvement of CO_2 adsorption and key intermediates stability, supporting In_2O_3 on the other metal oxides is considered to be extremely useful, especially the combination of In_2O_3 with ZrO_2 support. ZrO_2 support is an excellent modifier for In_2O_3 to promote the concentration of oxygen vacancy, enhance the interaction with CO_2, and stabilize the key intermediates. The structure–activity relationship of In_2O_3/ZrO_2 can be concluded as follows: high surface and dispersion of In_2O_3 to prevent sintering and strong interaction of In_2O_3 and ZrO_2 (i.e., solid solution m-ZrO_2:In) from preventing the over-reduction of In_2O_3, generate more active In-oxygen vacancy (V_o)-Zr sites for activating CO_2 and stabilizing key formate intermediates, and also form electron-rich In_2O_3 (electron transfer from ZrO_2 to In_2O_3) to facilitate the dissociation of hydrogen. In addition, the phase state of ZrO_2 support greatly affects the catalytic activity of In_2O_3/ZrO_2, and different from amorphous ZrO_2 and tetragonal ZrO_2, the interaction between monoclinic ZrO_2 and In_2O_3 nanoparticles can impel atomical dispersion of In^{2+}/In^{3+} into m-ZrO_2 lattice to form solid solution m-ZrO_2:In, which prevented the over-reduction of In species and stabilized the active In-oxygen vacancy-Zr sites to facilitate CO_2 conversion into methanol.

Although the research of In_2O_3-based catalysts for CO_2 hydrogenation to methanol has made substantial headway recently, several issues remain to be addressed in future studies. For instance, it is urgent to reveal the evolutionary process of active sites under real reaction conditions, which is extremely crucial to establish a more intuitive and reliable structure–activity relationship for designing In_2O_3-based catalysts. In addition, the catalytic mechanism over In_2O_3-based catalysts is usually proposed by theoretical study-based DFT calculation at present; however, the validity in practical applications is rather challenging. On the one hand, the microscopic reaction process (molecular level) could not be observed through experiments to verify its validity. On the other hand, the DFT calculation is unable to restore the real experimental conditions (i.e., species of active sites, mass transfer, etc.), therefore resulting in the difference between the theoretical reaction pathway and the actual reaction pathway. In order to obtain the evolutionary process of active sites and valid reaction mechanism, two considerable methods should be highlighted in future studies as follows: (1) making more efforts to analyze and identify the species of key intermediates by comprehensive in situ characterization technology (i.e., in situ DRIFTS, in situ XPS, etc.) and kinetic investigation; (2) combining DFT calculations with other simulation methods (i.e., computational fluid dynamics (CFD), kinetic Monte Carlo (KMC), etc.) to build more realistic models for theoretical study. Furthermore, from the point view of practical application, it is extremely necessary to reveal the deactivation mechanisms and enhance catalytic stability of In_2O_3-based catalysts in converting CO_2 into methanol, so more attention should be paid to the issues of sintering and the structural evolution monitored by in situ/operando spectroscopic techniques. Overall, this review mainly summarized the regulation and modification of active sites of In_2O_3-based catalysts to facilitate the activation of reactants and stabilization of intermediates in CO_2 hydrogenation, which is conducive to the design of more efficient In_2O_3-based catalysts for the highly selective transformation of CO_2 to methanol in future studies, realizing the resource utilization of CO_2.

Author Contributions: Conceptualization, D.C. and G.Z.; validation, Y.C., K.B.T. and G.Z.; formal analysis, Y.C.; writing—original draft preparation, D.C.; writing—review and editing, K.B.T. and G.Z.; visualization, K.B.T.; supervision, G.Z. All authors have read and agreed to the published version of the manuscript.

Funding: This work was supported by the National Natural Science Foundation of China (Nos. U21A20324 and 22278167), the Natural Science Foundation of Fujian Province (Nos. 2022J01312 and 2021J06026), and Start-Up Scientific Research Funds for Newly Recruited Talents of Huaqiao University (No. 605-50Y20015).

Institutional Review Board Statement: Not applicable.

Informed Consent Statement: Not applicable.

Data Availability Statement: Not applicable.

Conflicts of Interest: The authors declare no conflict of interest.

References

1. Yue, Y.; Huang, Z.; Cai, D.; Ullah, S.; Ibrahim, A.-R.; Yang, X.; Huang, J.; Zhan, G. Fabrication of multi-layered Co_3O_4/ZnO nanocatalysts for spectroscopic visualization: Effect of spatial positions on CO_2 hydrogenation performance. *Fuel* **2022**, *321*, 124042. [CrossRef]
2. Tan, K.B.; Zhan, G.; Sun, D.; Huang, J.; Li, Q. The development of bifunctional catalysts for carbon dioxide hydrogenation to hydrocarbons via the methanol route: From single component to integrated components. *J. Mater. Chem. A* **2021**, *9*, 5197–5231. [CrossRef]
3. Li, W.; Wang, K.; Zhan, G.; Huang, J.; Li, Q. Hydrogenation of CO_2 to Dimethyl Ether over Tandem Catalysts Based on Biotemplated Hierarchical ZSM-5 and Pd/ZnO. *ACS Sustain. Chem. Eng.* **2020**, *8*, 14058–14070. [CrossRef]
4. Boot-Handford, M.E.; Abanades, J.C.; Anthony, E.J.; Blunt, M.J.; Brandani, S.; Mac Dowell, N.; Fernández, J.R.; Ferrari, M.-C.; Gross, R.; Hallett, J.P.; et al. Carbon capture and storage update. *Energy Environ. Sci.* **2014**, *7*, 130–189. [CrossRef]
5. Song, M.; Huang, Z.; Chen, B.; Liu, S.; Ullah, S.; Cai, D.; Zhan, G. Reduction treatment of nickel phyllosilicate supported Pt nanocatalysts determining product selectivity in CO_2 hydrogenation. *J. CO_2 Util.* **2021**, *52*, 101674. [CrossRef]
6. Liu, S.; Song, M.; Cha, X.; Hu, S.; Cai, D.; Li, W.; Zhan, G. Nickel phyllosilicates functionalized with graphene oxide to boost CO selectivity in CO_2 hydrogenation. *Sep. Purif. Technol.* **2022**, *287*, 120555. [CrossRef]
7. Wang, L.; Wang, D.; Li, Y. Single-atom catalysis for carbon neutrality. *Carbon Energy* **2022**, *4*, 1021–1079. [CrossRef]
8. Liu, Z.; Deng, Z.; He, G.; Wang, H.; Zhang, X.; Lin, J.; Qi, Y.; Liang, X. Challenges and opportunities for carbon neutrality in China. *Nat. Rev. Earth Environ.* **2021**, *3*, 141–155. [CrossRef]
9. Calzadiaz-Ramirez, L.; Meyer, A.S. Formate dehydrogenases for CO_2 utilization. *Curr. Opin. Biotechnol.* **2022**, *73*, 95–100. [CrossRef]
10. Kim, J.; Seong, A.; Yang, Y.; Joo, S.; Kim, C.; Jeon, D.H.; Dai, L.; Kim, G. Indirect surpassing CO_2 utilization in membrane-free CO_2 battery. *Nano Energy* **2021**, *82*, 105741. [CrossRef]
11. Castro, S.; Albo, J.; Irabien, A. Photoelectrochemical Reactors for CO_2 Utilization. *ACS Sustain. Chem. Eng.* **2018**, *6*, 15877–15894. [CrossRef]
12. Mikulčić, H.; Ridjan Skov, I.; Dominković, D.F.; Wan Alwi, S.R.; Manan, Z.A.; Tan, R.; Duić, N.; Hidayah Mohamad, S.N.; Wang, X. Flexible Carbon Capture and Utilization technologies in future energy systems and the utilization pathways of captured CO_2. *Renew Sust. Energ. Rev.* **2019**, *114*, 109338. [CrossRef]
13. Reis Machado, A.S.; Nunes da Ponte, M. CO_2 capture and electrochemical conversion. *Curr. Opin. Green Sustain. Chem.* **2018**, *11*, 86–90. [CrossRef]
14. Ren, M.; Zhang, Y.; Wang, X.; Qiu, H. Catalytic Hydrogenation of CO_2 to Methanol: A Review. *Catalysts* **2022**, *12*, 403. [CrossRef]
15. Murthy, P.S.; Liang, W.; Jiang, Y.; Huang, J. Cu-Based Nanocatalysts for CO_2 Hydrogenation to Methanol. *Energy Fuels* **2021**, *35*, 8558–8584. [CrossRef]
16. Bowker, M. Methanol Synthesis from CO_2 Hydrogenation. *ChemCatChem* **2019**, *11*, 4238–4246. [CrossRef]
17. Choi, E.J.; Lee, Y.H.; Lee, D.-W.; Moon, D.-J.; Lee, K.-Y. Hydrogenation of CO_2 to methanol over Pd–Cu/CeO_2 catalysts. *Mol. Catal.* **2017**, *434*, 146–153. [CrossRef]
18. Zhao, F.; Fan, L.; Xu, K.; Hua, D.; Zhan, G.; Zhou, S.-F. Hierarchical sheet-like Cu/Zn/Al nanocatalysts derived from LDH/MOF composites for CO_2 hydrogenation to methanol. *J. CO_2 Util.* **2019**, *33*, 222–232. [CrossRef]
19. Li, Y.; Na, W.; Wang, H.; Gao, W. Hydrogenation of CO_2 to methanol over Au–CuO/SBA-15 catalysts. *J. Porous Mater.* **2016**, *24*, 591–599. [CrossRef]
20. García-Trenco, A.; Regoutz, A.; White, E.R.; Payne, D.J.; Shaffer, M.S.P.; Williams, C.K. PdIn intermetallic nanoparticles for the Hydrogenation of CO_2 to Methanol. *Appl. Catal. B* **2018**, *220*, 9–18. [CrossRef]
21. Wang, J.; Zhang, G.; Zhu, J.; Zhang, X.; Ding, F.; Zhang, A.; Guo, X.; Song, C. CO_2 Hydrogenation to Methanol over In_2O_3-Based Catalysts: From Mechanism to Catalyst Development. *ACS Catal.* **2021**, *11*, 1406–1423. [CrossRef]

22. Zhong, J.; Yang, X.; Wu, Z.; Liang, B.; Huang, Y.; Zhang, T. State of the art and perspectives in heterogeneous catalysis of CO_2 hydrogenation to methanol. *Chem. Soc. Rev.* **2020**, *49*, 1385–1413. [CrossRef] [PubMed]
23. Tian, G.; Wu, Y.; Wu, S.; Huang, S.; Gao, J. Solid-State Synthesis of Pd/In_2O_3 Catalysts for CO_2 Hydrogenation to Methanol. *Catal. Lett.* **2022**, *153*, 903–910. [CrossRef]
24. Choi, H.; Oh, S.; Trung Tran, S.B.; Park, J.Y. Size-controlled model Ni catalysts on Ga_2O_3 for CO_2 hydrogenation to methanol. *J. Catal.* **2019**, *376*, 68–76. [CrossRef]
25. Poerjoto, A.J.; Ashok, J.; Dewangan, N.; Kawi, S. The role of lattice oxygen in CO_2 hydrogenation to methanol over $La_{1-x}Sr_xCuO$ catalysts. *J. CO_2 Util.* **2021**, *47*, 101498. [CrossRef]
26. Kothandaraman, J.; Dagle, R.A.; Dagle, V.L.; Davidson, S.D.; Walter, E.D.; Burton, S.D.; Hoyt, D.W.; Heldebrant, D.J. Condensed-phase low temperature heterogeneous hydrogenation of CO_2 to methanol. *Catal. Sci. Technol.* **2018**, *8*, 5098–5103. [CrossRef]
27. Frusteri, L.; Cannilla, C.; Todaro, S.; Frusteri, F.; Bonura, G. Tailoring of Hydrotalcite-Derived Cu-Based Catalysts for CO_2 Hydrogenation to Methanol. *Catalysts* **2019**, *9*, 1058. [CrossRef]
28. Din, I.U.; Shaharun, M.S.; Naeem, A.; Tasleem, S.; Johan, M.R. Carbon nanofiber-based copper/zirconia catalyst for hydrogenation of CO_2 to methanol. *J. CO_2 Util.* **2017**, *21*, 145–155. [CrossRef]
29. Zhang, X.; Liu, J.-X.; Zijlstra, B.; Filot, I.A.W.; Zhou, Z.; Sun, S.; Hensen, E.J.M. Optimum Cu nanoparticle catalysts for CO_2 hydrogenation towards methanol. *Nano Energy* **2018**, *43*, 200–209. [CrossRef]
30. Gutterod, E.S.; Lazzarini, A.; Fjermestad, T.; Kaur, G.; Manzoli, M.; Bordiga, S.; Svelle, S.; Lillerud, K.P.; Skulason, E.; Oien-Odegaard, S.; et al. Hydrogenation of CO_2 to Methanol by Pt Nanoparticles Encapsulated in UiO-67: Deciphering the Role of the Metal-Organic Framework. *J. Am. Chem. Soc.* **2020**, *142*, 999–1009. [CrossRef]
31. Toyao, T.; Kayamori, S.; Maeno, Z.; Siddiki, S.M.A.H.; Shimizu, K.-i. Heterogeneous Pt and MoO_x Co-Loaded TiO_2 Catalysts for Low-Temperature CO_2 Hydrogenation To Form CH_3OH. *ACS Catal.* **2019**, *9*, 8187–8196. [CrossRef]
32. Ojelade, O.A.; Zaman, S.F.; Daous, M.A.; Al-Zahrani, A.A.; Malik, A.S.; Driss, H.; Shterk, G.; Gascon, J. Optimizing Pd:Zn molar ratio in $PdZn/CeO_2$ for CO_2 hydrogenation to methanol. *Appl Catal. A-Gen.* **2019**, *584*, 117185. [CrossRef]
33. Geng, F.; Bonita, Y.; Jain, V.; Magiera, M.; Rai, N.; Hicks, J.C. Bimetallic Ru–Mo Phosphide Catalysts for the Hydrogenation of CO_2 to Methanol. *Ind. Eng. Chem. Res.* **2020**, *59*, 6931–6943. [CrossRef]
34. Feng, W.-H.; Yu, M.-M.; Wang, L.-J.; Miao, Y.-T.; Shakouri, M.; Ran, J.; Hu, Y.; Li, Z.; Huang, R.; Lu, Y.-L.; et al. Insights into Bimetallic Oxide Synergy during Carbon Dioxide Hydrogenation to Methanol and Dimethyl Ether over $GaZrO_x$ Oxide Catalysts. *ACS Catal.* **2021**, *11*, 4704–4711. [CrossRef]
35. Sha, F.; Tang, C.; Tang, S.; Wang, Q.; Han, Z.; Wang, J.; Li, C. The promoting role of Ga in $ZnZrO_x$ solid solution catalyst for CO_2 hydrogenation to methanol. *J. Catal.* **2021**, *404*, 383–392. [CrossRef]
36. Lee, K.; Anjum, U.; Araújo, T.P.; Mondelli, C.; He, Q.; Furukawa, S.; Pérez-Ramírez, J.; Kozlov, S.M.; Yan, N. Atomic Pd-promoted ZnZrO solid solution catalyst for CO_2 hydrogenation to methanol. *Appl. Catal. B* **2022**, *304*, 120994. [CrossRef]
37. Xu, D.; Hong, X.; Liu, G. Highly dispersed metal doping to ZnZr oxide catalyst for CO_2 hydrogenation to methanol: Insight into hydrogen spillover. *J. Catal.* **2021**, *393*, 207–214. [CrossRef]
38. Sun, K.; Fan, Z.; Ye, J.; Yan, J.; Ge, Q.; Li, Y.; He, W.; Yang, W.; Liu, C.-j. Hydrogenation of CO_2 to methanol over In_2O_3 catalyst. *J. CO_2 Util.* **2015**, *12*, 1–6. [CrossRef]
39. Ghosh, S.; Sebastian, J.; Olsson, L.; Creaser, D. Experimental and kinetic modeling studies of methanol synthesis from CO_2 hydrogenation using In_2O_3 catalyst. *Chem. Eng. J.* **2021**, *416*, 129120. [CrossRef]
40. Baumgarten, R.; Naumann d'Alnoncourt, R.; Lohr, S.; Gioria, E.; Frei, E.; Fako, E.; De, S.; Boscagli, C.; Drieß, M.; Schunk, S.; et al. Quantification and Tuning of Surface Oxygen Vacancies for the Hydrogenation of CO_2 on Indium Oxide Catalysts. *Chem. Ing. Tech.* **2022**, *94*, 1765–1775. [CrossRef]
41. Medina, J.C.; Figueroa, M.; Manrique, R.; Rodríguez Pereira, J.; Srinivasan, P.D.; Bravo-Suárez, J.J.; Baldovino Medrano, V.G.; Jiménez, R.; Karelovic, A. Catalytic consequences of Ga promotion on Cu for CO_2 hydrogenation to methanol. *Catal. Sci. Technol.* **2017**, *7*, 3375–3387. [CrossRef]
42. Chou, C.-Y.; Lobo, R.F. Direct conversion of CO_2 into methanol over promoted indium oxide-based catalysts. *Appl Catal. A-Gen.* **2019**, *583*, 117144. [CrossRef]
43. Fichtl, M.B.; Schlereth, D.; Jacobsen, N.; Kasatkin, I.; Schumann, J.; Behrens, M.; Schlögl, R.; Hinrichsen, O. Kinetics of deactivation on $Cu/ZnO/Al_2O_3$ methanol synthesis catalysts. *Appl Catal. A-Gen.* **2015**, *502*, 262–270. [CrossRef]
44. Sun, J.T.; Metcalfe, I.S.; Sahibzada, M. Deactivation of $Cu/ZnO/Al_2O_3$ Methanol Synthesis Catalyst by Sintering. *Ind. Eng. Chem. Res.* **1999**, *38*, 3868–3872. [CrossRef]
45. Wang, W.; Wang, S.; Ma, X.; Gong, J. Recent advances in catalytic hydrogenation of carbon dioxide. *Chem. Soc. Rev.* **2011**, *40*, 3703–3727. [CrossRef]
46. Porosoff, M.D.; Yan, B.; Chen, J.G. Catalytic reduction of CO_2 by H_2 for synthesis of CO, methanol and hydrocarbons: Challenges and opportunities. *Energy Environ. Sci.* **2016**, *9*, 62–73. [CrossRef]
47. Huang, Z.L.; Yuan, Y.J.; Song, M.M.; Hao, Z.M.; Xiao, J.R.; Cai, D.R.; Ibrahim, A.R.; Zhan, G.W. CO_2 hydrogenation over mesoporous $Ni-Pt/SiO_2$ nanorod catalysts: Determining CH_4/CO selectivity by surface ratio of Ni/Pt. *Chem. Eng. Sci.* **2022**, *247*, 117106. [CrossRef]

48. Li, W.; Wang, K.; Huang, J.; Liu, X.; Fu, D.; Huang, J.; Li, Q.; Zhan, G. M_xO_y-ZrO_2 (M = Zn, Co, Cu) Solid Solutions Derived from Schiff Base-Bridged UiO-66 Composites as High-Performance Catalysts for CO_2 Hydrogenation. *ACS Appl. Mater. Interfaces* **2019**, *11*, 33263–33272. [CrossRef]
49. Sha, F.; Tang, S.; Tang, C.; Feng, Z.; Wang, J.; Li, C. The role of surface hydroxyls on $ZnZrO_x$ solid solution catalyst in CO_2 hydrogenation to methanol. *Chin. J. Catal.* **2023**, *45*, 162–173. [CrossRef]
50. Pinheiro Araújo, T.; Morales-Vidal, J.; Zou, T.; Agrachev, M.; Verstraeten, S.; Willi, P.O.; Grass, R.N.; Jeschke, G.; Mitchell, S.; López, N.; et al. Design of Flame-Made $ZnZrO_x$ Catalysts for Sustainable Methanol Synthesis from CO_2. *Adv. Energy Mater.* **2023**, 2204122. [CrossRef]
51. Wang, J.; Li, G.; Li, Z.; Tang, C.; Feng, Z.; An, H.; Liu, H.; Liu, T.; Li, C. A highly selective and stable ZnO-ZrO_2 solid solution catalyst for CO_2 hydrogenation to methanol. *Sci. Adv.* **2017**, *3*, e1701290. [CrossRef]
52. Sadeghinia, M.; Rezaei, M.; Kharat, A.N.; Jorabchi, M.N.; Nematollahi, B.; Zareiekordshouli, F. Effect of In_2O_3 on the structural properties and catalytic performance of the CuO/ZnO/Al_2O_3 catalyst in CO_2 and CO hydrogenation to methanol. *Mol. Catal.* **2020**, *484*, 110776. [CrossRef]
53. Ye, J.Y.; Liu, C.J.; Mei, D.H.; Ge, Q.F. Active Oxygen Vacancy Site for Methanol Synthesis from CO_2 Hydrogenation on In_2O_3(110): A DFT Study. *ACS Catal.* **2013**, *3*, 1296–1306. [CrossRef]
54. Qin, B.; Li, S. First principles investigation of dissociative adsorption of H_2 during CO_2 hydrogenation over cubic and hexagonal In_2O_3 catalysts. *PCCP* **2020**, *22*, 3390–3399. [CrossRef]
55. Wang, L.; Dong, Y.; Yan, T.; Hu, Z.; Jelle, A.A.; Meira, D.M.; Duchesne, P.N.; Loh, J.Y.Y.; Qiu, C.; Storey, E.E.; et al. Black indium oxide a photothermal CO_2 hydrogenation catalyst. *Nat. Commun.* **2020**, *11*, 2432. [CrossRef]
56. Lorenz, H.; Jochum, W.; Klötzer, B.; Stöger-Pollach, M.; Schwarz, S.; Pfaller, K.; Penner, S. Novel methanol steam reforming activity and selectivity of pure In_2O_3. *Appl. Catal. A-Gen.* **2008**, *347*, 34–42. [CrossRef]
57. Bielz, T.; Lorenz, H.; Amann, P.; Klötzer, B.; Penner, S. Water–Gas Shift and Formaldehyde Reforming Activity Determined by Defect Chemistry of Polycrystalline In_2O_3. *J. Phys. Chem. C* **2011**, *115*, 6622–6628. [CrossRef]
58. Martin, O.; Martin, A.J.; Mondelli, C.; Mitchell, S.; Segawa, T.F.; Hauert, R.; Drouilly, C.; Curulla-Ferre, D.; Perez-Ramirez, J. Indium Oxide as a Superior Catalyst for Methanol Synthesis by CO_2 Hydrogenation. *Angew. Chem. Int. Ed.* **2016**, *55*, 6261–6265. [CrossRef]
59. Frei, M.S.; Capdevila-Cortada, M.; Garcia-Muelas, R.; Mondelli, C.; Lopez, N.; Stewart, J.A.; Ferre, D.C.; Perez-Ramirez, J. Mechanism and microkinetics of methanol synthesis via CO_2 hydrogenation on indium oxide. *J. Catal.* **2018**, *361*, 313–321. [CrossRef]
60. Tsoukalou, A.; Abdala, P.M.; Stoian, D.; Huang, X.; Willinger, M.G.; Fedorov, A.; Muller, C.R. Structural Evolution and Dynamics of an In_2O_3 Catalyst for CO_2 Hydrogenation to Methanol: An *Operando* XAS-XRD and In Situ TEM Study. *J. Am. Chem. Soc.* **2019**, *141*, 13497–13505. [CrossRef]
61. Sun, K.; Rui, N.; Zhang, Z.; Sun, Z.; Ge, Q.; Liu, C.-J. A highly active Pt-In_2O_3 catalyst for CO_2 hydrogenation to methanol with enhanced stability. *Green Chem.* **2020**, *22*, 5059–5066. [CrossRef]
62. Yang, B.; Li, L.; Jia, Z.; Liu, X.; Zhang, C.; Guo, L. Comparative study of CO_2 hydrogenation to methanol on cubic bixbyite-type and rhombohedral corundum-type indium oxide. *Chin. Chem. Lett.* **2020**, *31*, 2627–2633. [CrossRef]
63. Dang, S.; Qin, B.; Yang, Y.; Wang, H.; Cai, J.; Han, Y.; Li, S.; Gao, P.; Sun, Y. Rationally designed indium oxide catalysts for CO_2 hydrogenation to methanol with high activity and selectivity. *Sci. Adv.* **2020**, *6*, eaaz2060. [CrossRef] [PubMed]
64. Shi, Z.; Tan, Q.; Wu, D. Mixed-Phase Indium Oxide as a Highly Active and Stable Catalyst for the Hydrogenation of CO_2 to CH_3OH. *Ind. Eng. Chem. Res.* **2021**, *60*, 3532–3542. [CrossRef]
65. Cao, A.; Wang, Z.; Li, H.; Nørskov, J.K. Relations between Surface Oxygen Vacancies and Activity of Methanol Formation from CO_2 Hydrogenation over In_2O_3 Surfaces. *ACS Catal.* **2021**, *11*, 1780–1786. [CrossRef]
66. Qin, B.; Zhou, Z.; Li, S.; Gao, P. Understanding the structure-performance relationship of cubic In_2O_3 catalysts for CO_2 hydrogenation. *J. CO_2 Util.* **2021**, *49*, 101543. [CrossRef]
67. Wang, W.; Chen, Y.; Zhang, M. Facet effect of In_2O_3 for methanol synthesis by CO_2 hydrogenation: A mechanistic and kinetic study. *Surf. Interfaces* **2021**, *25*, 101244. [CrossRef]
68. Rui, N.; Wang, Z.; Sun, K.; Ye, J.; Ge, Q.; Liu, C.-j. CO_2 hydrogenation to methanol over Pd/In_2O_3: Effects of Pd and oxygen vacancy. *Appl. Catal. B* **2017**, *218*, 488–497. [CrossRef]
69. Cai, Z.; Dai, J.; Li, W.; Tan, K.B.; Huang, Z.; Zhan, G.; Huang, J.; Li, Q. Pd Supported on MIL-68(In)-Derived In_2O_3 Nanotubes as Superior Catalysts to Boost CO_2 Hydrogenation to Methanol. *ACS Catal.* **2020**, *10*, 13275–13289. [CrossRef]
70. Guanfeng, T.; Youqing, W.; Shiyong, W.; Sheng, H.; Jinsheng, G. CO_2 hydrogenation to methanol over Pd/MnO/In_2O_3 catalyst. *J. Environ. Chem. Eng.* **2021**, *10*, 106965. [CrossRef]
71. Han, Z.; Tang, C.; Wang, J.; Li, L.; Li, C. Atomically dispersed Pt^{n+} species as highly active sites in Pt/In_2O_3 catalysts for methanol synthesis from CO_2 hydrogenation. *J. Catal.* **2021**, *394*, 236–244. [CrossRef]
72. Wang, J.; Sun, K.; Jia, X.; Liu, C.-j. CO_2 hydrogenation to methanol over Rh/In_2O_3 catalyst. *Catal. Today* **2021**, *365*, 341–347. [CrossRef]
73. Dostagir, N.H.M.D.; Thompson, C.; Kobayashi, H.; Karim, A.M.; Fukuoka, A.; Shrotri, A. Rh promoted In_2O_3 as a highly active catalyst for CO_2 hydrogenation to methanol. *Catal. Sci. Technol.* **2020**, *10*, 8196–8202. [CrossRef]

74. Qinglei, W.; Chenyang, S.; Ning, R.; Kaihang, S.; Chang-jun, L. Experimental and theoretical studies of CO_2 hydrogenation to methanol on Ru/In_2O_3. *J. CO_2 Util.* **2021**, *53*, 101720. [CrossRef]
75. Rui, N.; Zhang, F.; Sun, K.; Liu, Z.; Xu, W.; Stavitski, E.; Senanayake, S.D.; Rodriguez, J.A.; Liu, C.-J. Hydrogenation of CO_2 to Methanol on a $Au^{\delta+}$–In_2O_{3-x} Catalyst. *ACS Catal.* **2020**, *10*, 11307–11317. [CrossRef]
76. Shen, C.; Sun, K.; Zhang, Z.; Rui, N.; Jia, X.; Mei, D.; Liu, C.-j. Highly Active Ir/In_2O_3 Catalysts for Selective Hydrogenation of CO_2 to Methanol: Experimental and Theoretical Studies. *ACS Catal.* **2021**, *11*, 4036–4046. [CrossRef]
77. Jia, X.; Sun, K.; Wang, J.; Shen, C.; Liu, C.-j. Selective hydrogenation of CO_2 to methanol over Ni/In_2O_3 catalyst. *J. Energy Chem.* **2020**, *50*, 409–415. [CrossRef]
78. Zhu, J.; Cannizzaro, F.; Liu, L.; Zhang, H.; Kosinov, N.; Filot, I.A.W.; Rabeah, J.; Bruckner, A.; Hensen, E.J.M. Ni-In Synergy in CO_2 Hydrogenation to Methanol. *ACS Catal.* **2021**, *11*, 11371–11384. [CrossRef]
79. Li, L.; Yang, B.; Gao, B.; Wang, Y.; Zhang, L.; Ishihara, T.; Qi, W.; Guo, L. CO_2 hydrogenation selectivity shift over In-Co binary oxides catalysts: Catalytic mechanism and structure-property relationship. *Chin. J. Catal.* **2022**, *43*, 862–876. [CrossRef]
80. Pustovarenko, A.; Dikhtiarenko, A.; Bavykina, A.; Gevers, L.; Ramírez, A.; Russkikh, A.; Telalovic, S.; Aguilar, A.; Hazemann, J.-L.; Ould-Chikh, S.; et al. Metal–Organic Framework-Derived Synthesis of Cobalt Indium Catalysts for the Hydrogenation of CO_2 to Methanol. *ACS Catal.* **2020**, *10*, 5064–5076. [CrossRef]
81. Shi, Z.; Pan, M.; Wei, X.; Wu, D. Cu-In intermetallic compounds as highly active catalysts for CH_3OH formation from CO_2 hydrogenation. *Int. J. Energy Res.* **2021**, *46*, 1285–1298. [CrossRef]
82. Yang, C.; Pei, C.; Luo, R.; Liu, S.; Wang, Y.; Wang, Z.; Zhao, Z.J.; Gong, J. Strong Electronic Oxide-Support Interaction over In_2O_3/ZrO_2 for Highly Selective CO_2 Hydrogenation to Methanol. *J. Am. Chem. Soc.* **2020**, *142*, 19523–19531. [CrossRef] [PubMed]
83. Chen, T.-y.; Cao, C.; Chen, T.-b.; Ding, X.; Huang, H.; Shen, L.; Cao, X.; Zhu, M.; Xu, J.; Gao, J.; et al. Unraveling Highly Tunable Selectivity in CO_2 Hydrogenation over Bimetallic In-Zr Oxide Catalysts. *ACS Catal.* **2019**, *9*, 8785–8797. [CrossRef]
84. Akkharaphatthawon, N.; Chanlek, N.; Cheng, C.K.; Chareonpanich, M.; Limtrakul, J.; Witoon, T. Tuning adsorption properties of $Ga_xIn_{2-x}O_3$ catalysts for enhancement of methanol synthesis activity from CO_2 hydrogenation at high reaction temperature. *Appl. Surf. Sci.* **2019**, *489*, 278–286. [CrossRef]
85. Regalado Vera, C.Y.; Manavi, N.; Zhou, Z.; Wang, L.-C.; Diao, W.; Karakalos, S.; Liu, B.; Stowers, K.J.; Zhou, M.; Luo, H.; et al. Mechanistic understanding of support effect on the activity and selectivity of indium oxide catalysts for CO_2 hydrogenation. *Chem. Eng. J.* **2021**, *426*, 131767. [CrossRef]
86. Frei, M.S.; Mondelli, C.; Cesarini, A.; Krumeich, F.; Hauert, R.; Stewart, J.A.; Curulla Ferré, D.; Pérez-Ramírez, J. Role of Zirconia in Indium Oxide-Catalyzed CO_2 Hydrogenation to Methanol. *ACS Catal.* **2019**, *10*, 1133–1145. [CrossRef]
87. Ye, J.; Liu, C.-j.; Mei, D.; Ge, Q. Methanol synthesis from CO_2 hydrogenation over a Pd_4/In_2O_3 model catalyst: A combined DFT and kinetic study. *J. Catal.* **2014**, *317*, 44–53. [CrossRef]
88. Cai, Z.; Huang, M.; Dai, J.; Zhan, G.; Sun, F.-l.; Zhuang, G.-L.; Wang, Y.; Tian, P.; Chen, B.; Ullah, S.; et al. Fabrication of Pd/In_2O_3 Nanocatalysts Derived from MIL-68(In) Loaded with Molecular Metalloporphyrin (TCPP(Pd)) Toward CO_2 Hydrogenation to Methanol. *ACS Catal.* **2022**, *12*, 709–723. [CrossRef]
89. Pan, T.; Zhongjie, C.; Guowu, Z.; Jiale, H.; Qingbiao, L. Preparation of supported In_2O_3/Pd nanocatalysts using natural pollen as bio-templates for CO_2 hydrogenation to methanol: Effect of acid-etching on template. *Mol. Catal.* **2021**, *516*, 111945. [CrossRef]
90. Bing Tan, K.; Tian, P.; Zhang, X.; Tian, J.; Zhan, G.; Huang, J.; Li, Q. Green synthesis of microspherical-confined nano-Pd/In_2O_3 integrated with H-ZSM-5 as bifunctional catalyst for CO_2 hydrogenation into dimethyl ether: A carbonized alginate templating strategy. *Sep. Purif. Technol.* **2022**, *297*, 121559. [CrossRef]
91. Frei, M.S.; Mondelli, C.; García-Muelas, R.; Kley, K.S.; Puértolas, B.; López, N.; Safonova, O.V.; Stewart, J.A.; Curulla Ferré, D.; Pérez-Ramírez, J. Atomic-scale engineering of indium oxide promotion by palladium for methanol production via CO_2 hydrogenation. *Nat. Commun.* **2019**, *10*, 3377. [CrossRef]
92. Jiang, H.; Lin, J.; Wu, X.; Wang, W.; Chen, Y.; Zhang, M. Efficient hydrogenation of CO_2 to methanol over Pd/In_2O_3/SBA-15 catalysts. *J. CO_2 Util.* **2020**, *36*, 33–39. [CrossRef]
93. Men, Y.-L.; Liu, Y.; Wang, Q.; Luo, Z.-H.; Shao, S.; Li, Y.-B.; Pan, Y.-X. Highly dispersed Pt-based catalysts for selective CO_2 hydrogenation to methanol at atmospheric pressure. *Chem. Eng. Sci.* **2019**, *200*, 167–175. [CrossRef]
94. Pinheiro Araújo, T.; Morales-Vidal, J.; Zou, T.; García-Muelas, R.; Willi, P.O.; Engel, K.M.; Safonova, O.V.; Faust Akl, D.; Krumeich, F.; Grass, R.N.; et al. Flame Spray Pyrolysis as a Synthesis Platform to Assess Metal Promotion in In_2O_3-Catalyzed CO_2 Hydrogenation. *Adv. Energy Mater.* **2022**, *12*, 2103707. [CrossRef]
95. Sun, K.; Zhang, Z.; Shen, C.; Rui, N.; Liu, C.-j. The feasibility study of the indium oxide supported silver catalyst for selective hydrogenation of CO_2 to methanol. *Green Energy Environ.* **2022**, *7*, 807–817. [CrossRef]
96. Shen, C.; Bao, Q.; Xue, W.; Sun, K.; Zhang, Z.; Jia, X.; Mei, D.; Liu, C.-j. Synergistic effect of the metal-support interaction and interfacial oxygen vacancy for CO_2 hydrogenation to methanol over Ni/In_2O_3 catalyst: A theoretical study. *J. Energy Chem.* **2022**, *65*, 623–629. [CrossRef]
97. Zhang, Z.; Shen, C.; Sun, K.; Liu, C.-J. Improvement in the activity of Ni/In_2O_3 with the addition of ZrO_2 for CO_2 hydrogenation to methanol. *Catal. Commun.* **2022**, *162*, 106386. [CrossRef]
98. Fang, T.; Liu, B.; Lian, Y.; Zhang, Z. Selective Methanol Synthesis from CO_2 Hydrogenation over an In_2O_3/Co/C-N Catalyst. *Ind. Eng. Chem. Res.* **2020**, *59*, 19162–19167. [CrossRef]

99. Stangeland, K.; Navarro, H.H.; Huynh, H.L.; Tucho, W.M.; Yu, Z. Tuning the interfacial sites between copper and metal oxides (Zn, Zr, In) for CO_2 hydrogenation to methanol. *Chem. Eng. Sci.* **2021**, *238*, 116603. [CrossRef]
100. Zhang, X.; Kirilin, A.V.; Rozeveld, S.; Kang, J.H.; Pollefeyt, G.; Yancey, D.F.; Chojecki, A.; Vanchura, B.; Blum, M. Support Effect and Surface Reconstruction in In_2O_3/m-ZrO_2 Catalyzed CO_2 Hydrogenation. *ACS Catal.* **2022**, *12*, 3868–3880. [CrossRef]
101. Numpilai, T.; Kidkhunthod, P.; Cheng, C.K.; Wattanakit, C.; Chareonpanich, M.; Limtrakul, J.; Witoon, T. CO_2 hydrogenation to methanol at high reaction temperatures over In_2O_3/ZrO_2 catalysts: Influence of calcination temperatures of ZrO_2 support. *Catal. Today* **2021**, *375*, 298–306. [CrossRef]
102. Tsoukalou, A.; Abdala, P.M.; Armutlulu, A.; Willinger, E.; Fedorov, A.; Müller, C.R. Operando X-ray Absorption Spectroscopy Identifies a Monoclinic ZrO_2:In Solid Solution as the Active Phase for the Hydrogenation of CO_2 to Methanol. *ACS Catal.* **2020**, *10*, 10060–10067. [CrossRef]
103. Tsoukalou, A.; Serykh, A.I.; Willinger, E.; Kierzkowska, A.; Abdala, P.M.; Fedorov, A.; Müller, C.R. Hydrogen dissociation sites on indium-based ZrO_2-supported catalysts for hydrogenation of CO_2 to methanol. *Catal. Today* **2022**, *387*, 38–46. [CrossRef]
104. Wei, Y.; Liu, F.; Ma, J.; Yang, C.; Wang, X.; Cao, J. Catalytic roles of In_2O_3 in ZrO_2-based binary oxides for CO_2 hydrogenation to methanol. *Mol. Catal.* **2022**, *525*, 112354. [CrossRef]
105. Salomone, F.; Sartoretti, E.; Ballauri, S.; Castellino, M.; Novara, C.; Giorgis, F.; Pirone, R.; Bensaid, S. CO_2 hydrogenation to methanol over Zr- and Ce-doped indium oxide. *Catal. Today* **2023**, accepted. [CrossRef]
106. Tian, G.; Wu, Y.; Wu, S.; Huang, S.; Gao, J. Influence of Mn and Mg oxides on the performance of In_2O_3 catalysts for CO_2 hydrogenation to methanol. *Chem. Phys. Lett.* **2022**, *786*, 139173. [CrossRef]